Title: Subclinical anxiety is associated with reduced self-distancing and enhanced guilt-related connectivity between anterior temporal and subgenual cingulate cortices

Michal Rafal Zareba [1], Ivan González-García [1], Marcos Ibáñez Montolio [1], Richard J. Binney [2], Paul Hoffman [3], Maya Visser [1]

[1] Neuropsychology and Functional Neuroimaging Group, Department of Basic and Clinical Psychology and Psychobiology, Jaume I University, 12071 Castellon de la Plana, Spain
[2] Department of Psychology and Bangor Imaging Unit, Bangor University, Gwynedd, LL57 2AS, United Kingdom
[3] School of Philosophy, Psychology & Language Sciences, University of Edinburgh, Edinburgh, EH8 9AD, United Kingdom

Correspondence: zareba@uji.es (MRZ)

Abstract

Excessive self-blaming emotions are commonly observed in anxiety disorders, with mounting evidence indicating the presence of qualitatively similar symptomatology in subclinical and clinical populations. Prior work points to a central role of the superior anterior temporal lobe (sATL) in the guilt processing circuitry, together with network organisation differences associated with subclinical anxiety. This study aimed to extend these findings by exploring links of trait-anxiety with (i) self-blaming emotions and associated behaviours, and (ii) guilt-dependent neural activity and connectivity. We also explored the role of resting-state fMRI in linking these phenomena. Increased anxiety was linked to stronger self-blaming emotions, and more pronounced self-attacking and hiding. When experiencing negative emotions about themselves (i.e. shame and self-anger), anxious individuals were also less likely to disengage from self-focused thoughts. These behavioural findings were paralleled by enhanced guilt-related connectivity between the left sATL and bilateral posterior subgenual cingulate cortex. The relevance of temporal lobe activity for self-blaming emotions was also evident in the resting-state data. Interestingly, while the approach-avoidance motivation towards guilt memories was unrelated to anxiety, this emotional dimension showed distinct contributions of the left and right sATL, with task-related activity of the former and connectivity of the latter associated with, respectively, more approach and avoidance. As such, the results of the current study link the self-blaming bias of anxious individuals to specific maladaptive patterns of behaviour. Furthermore, the work provides robust evidence for the important role of ATL-related circuitry in guilt processing, supporting its broader involvement in social conceptual processing.

Keywords

anxiety; guilt; self-blame; approach-avoidance motivation; fMRI

1. Introduction

The growing prevalence of mood and anxiety disorders worldwide, a crisis that has accelerated in the years following the COVID-19 pandemic (Yuan et al., 2022), is a major challenge for modern society, as it comes with a high economic burden. Mental health problems significantly impact individual quality of life, with social difficulties being amongst the most often reported complaints. As navigating the complex world of interpersonal interactions is a key element of our everyday functioning, understanding the processes contributing to the emergence of these hardships is crucial in that it can inform novel, evidence-based strategies for improving social functioning of the affected individuals or preventing their development in the first place.

Although self-blaming emotions, such as guilt, are a well established characteristic of mood and anxiety disorders (Beck, 1963; Cândea and Szentagotai-Tătar, 2018), they only recently gained attention from the neuroscientific community. The self-blaming bias in major depressive disorder (MDD) patients has been linked to maladaptive behaviours, such as attacking oneself and being socially avoidant despite not having committed any wrongdoing (Duan et al., 2021; Duan et al., 2023). As for its neural basis, a number of neuroimaging studies highlighted the role of the right superior anterior temporal lobe regions involved in social semantics (sATL; Zahn et al., 2007; Thye et al., 2024). Specifically, reduced connectivity of the sATL with dorsolateral prefrontal cortex and ventral striatum during guilt processing was associated with the overgeneralisation of self-blaming emotions in in MDD patients (Green et al., 2013), while its coupling with subgenual anterior cingulate cortex (sgACC) was consistently found to be predictive of treatment response (Lythe et al., 2015; Zahn et al., 2019; Jaeckle et at., 2023; Fennema et al., 2023). Importantly, the connectivity with anterior and posterior parts of the sgACC, linked to social agency and affiliative processing, respectively (Zahn, 2025), was found to be differentially associated with depression progression, indicating that studying their coupling separately might provide insights into alterations in distinct guilt-related processes.

Despite the fact that anxious individuals, similarly to MDD patients, display elevated guilt proneness (Cândea and Szentagotai-Tătar, 2018), the behavioural and neural patterns associated with self-blaming in this group remain largely unexplored (González-García and Visser, 2023). In recent years it has been demonstrated that both subclinical and clinical anxious populations exhibit a comparable set of symptoms and similar underlying changes in neural activity (Besteher et al. 2017), suggesting that biologically-informed symptom-based models of mental health disorders may be more useful clinically than the current categorical classifications based on DSM-5-TR (Kas et al., 2025). For example, we demonstrated that the self-blaming tendency of subclinically anxious individuals was primarily related to increased functional contributions of the left sATL to the guilt processing circuitry, disconnection of the inferior frontal and insular regions involved in cognitive emotion regulation, and a network structural architecture favouring local information processing (Zareba et al., 2024a). Nevertheless, it still remains unknown whether the self-blaming bias observed in subclinically anxious individuals is associated with similar maladaptive behaviours and alterations in neural correlates of guilt experiences as previously reported in MDD patients. Likewise, despite the fact that both MDD and anxiety disorders patients are often prescribed pharmacotherapies targeting neuromodulatory brain systems, such as serotonin (5-HT), dopamine (DA) and norepinephrine (NE), the neural mechanisms through which these drugs may affect guilt-related symptomatology remain elusive (Kanen et al., 2021). With the anticipated shift in the paradigm towards personalised psychiatric treatments (Kas et al., 2025), understanding whether particular symptomatology has universal, transdiagnostic underpinnings is essential as such knowledge might help determine the most optimal therapeutic choices.

Therefore, we set out to thoroughly investigate the mechanisms behind self-blaming bias of subclinically anxious individuals, combining behavioural paradigms with functional magnetic

resonance imaging (fMRI). We used the Moral Sentiment and Action Tendencies task (MSAT; Zahn et al., 2015; Duan et al., 2023) to study blame-related social feelings and associated action tendencies, and their dependency on whether one is the performer or a recipient of inappropriate social actions (i.e. self- and other-agency). We expected to replicate prior findings in anxious individuals and observe a higher prevalence of negative social feelings towards oneself (e.g., guilt; Cândea and Szentagotai-Tătar, 2018). As the sense of agency plays a key role in the emergence of guilt (Caspar et al., 2020), we additionally expected this phenomenon to be more pronounced on the self-agency trials. Regarding the action tendencies, we hypothesised that higher levels of anxiety would be associated with increased hiding (social avoidance) and self-attacking, similarly to MDD patients (Duan et al., 2021; Duan et al., 2023), and that these observations will be particularly prominent on trials where one reports feeling guilty.

In addition, a subset of participants underwent fMRI while recalling autobiographical guilt memories. We expected subclinically anxious individuals to report more avoidance towards their guilt memories, and perceive these events as more salient. On the neural level, we hypothesised that these associations would be paralleled by increased guilt-dependent coupling between the sATL, which encodes meaning of social stimuli (Zahn et al., 2007; Binney et al., 2016), and posterior sgACC, which is involved in social affiliative processing (Zahn, 2025), mirroring the previous results in MDD patients (Lythe et al., 2015; Jaeckle et al., 2023).

Building on our work using graph theory (Zareba et al., 2024a), we aimed to characterise in greater detail the neural correlates of self-blaming emotions, this time using complementary voxel-wise methodology. We obtained resting-state fMRI data, calculated measures of brain activity and connectivity, and finally correlated them with strength of individual self-blaming emotions from the MSAT task (Zahn et al., 2015; Duan et al., 2023), expecting to observe statistically significant associations within the same set of regions as activated by the guilt recollection task deployed in this study, and particularly in the ATL (Zareba et al., 2024a).

Last but not least, to increase our understanding of how alterations in the neurotransmission strength within the modulatory brain networks could contribute to guilt symptomatology, we performed an exploratory hypothesis-generating analysis investigating how the guilt processing-evoked brain activity in our study was associated with the normative distribution of receptors and transporters belonging to such systems, deriving the latter information from publicly available atlases (Hansen et al., 2022; Gryglewski et al., 2018). Apart from the aforementioned 5-HT, DA and NE neurotransmission typically targeted in anxiety and MDD pharmacotherapy, we additionally explored the potential role of oxytocin (OXT), given the evidence for its crucial contributions to guilt processing (Li and Zu, 2024; Zheng et al., 2024).

2. Methods

The current study included a behavioural task, fMRI with a task on guilt processing, and resting-state fMRI. It adhered to the ethical standards of the Declaration of Helsinki and was approved by the local ethics committee (CEISH/07/2022). Participants provided informed consent prior to participation and were remunerated at a rate of 10 euros per hour.

2.1. Moral Sentiment and Action Tendencies Task (MSAT)

2.1.1. Participants

The MSAT task was performed by 140 healthy volunteers recruited mainly from the university community via local announcements and word of mouth. As the participants were also meant to subsequently undergo magnetic resonance imaging (MRI), the typical inclusion criteria for MRI studies were applied: right-handedness as assessed by the Edinburgh Handedness Inventory

(Oldfield, 1971), normal or corrected to normal vision, no history of neurological and psychiatric disorders, and not taking any psychotropic medication. Three measures of anxiety and associated facets were applied: State-Trait Anxiety Inventory (STAI; Spielberger, 1989), Sensitivity to Punishment and Sensitivity to Reward Questionnaire (SCSRQ; Torrubia et al., 2001) and Behavioral Inhibition and Behavioral Activation System (BIS/BAS; Carver and White, 1994), following the recommendation to assess symptomatology across several scales to increase results reliability and replicability (Fried and Nesse, 2015). For each participant, we calculated a composite score of anxiety by standardising (Z-score) their scores for trait-anxiety, sensitivity to punishment and behavioural inhibition system, and adding them all together. When recruiting for the study, we ensured we enrolled volunteers with a wide range of anxiety levels to ensure sufficient variability in the cohort. The characteristics of the sample are provided in Table 1.

Table 1. Demographic and psychological characteristics of the participants who performed the Moral Sentiment and Action Tendencies Task (MSAT).

Variable	Mean ± standard deviation	Possible range
Sex	87 females, 53 males	not applicable
Age	22.56 ± 4.07	not applicable
Trait-anxiety	23.31 ± 12.30	0-60
Sensitivity to punishment	12.66 ± 5.94	0-24
Behavioral inhibition system	22.19 ± 4.04	7-28

2.1.2. Task description

The MSAT task began with a screen asking participants to provide their name and the name of their same-sex best friend with whom they had no family or romantic bonds. Subsequently, they answered a question concerning how close they felt to their friend using a Likert-scale with 7 discrete levels (1 - not at all, 7 - very close). Only participants reporting feeling sufficiently close to their friends (i.e. ≥ 4) were included in the experiment. The value was missing for 1 subject, and 7 participants indicated not feeling sufficiently close to their friend, yielding the aforementioned final sample of 140 individuals.

In the main part of the task, participants were asked to imagine 54 hypothetical scenarios (27 behaviours repeated across 2 agency conditions) in which they (self-agency) or their friend (other-agency) were behaving counter to social and moral values, with the other person being the recipient of the action (e.g. “Michal is being bossy towards Marcos”). For each of such scenarios, subjects were asked how strongly they would blame themselves and their friends in the described situation (Likert scale ranging from 1 (not at all) to 7 (a lot)). Additionally, they were asked what emotion they would feel most strongly with the available choices being four self-blaming emotions (i.e. guilt, shame, contempt/disgust towards self and indignation/anger towards self), two other-blaming emotions (i.e. contempt/disgust towards the friend and indignation/anger towards the friend), as well as no/other emotion. At the end of the trial, the subjects were presented with a choice of 7 actions that they would most likely undertake in the particular scenario: feeling like verbally or physically attacking/punishing themselves, feeling like creating distance from themselves, feeling like hiding, feeling like apologising/fixing what they

have done, feeling like verbally or physically attacking/punishing their friend, feel like creating distance from their best friend, as well as no/other action.

2.1.3. Group-level analysis

All the described analyses were performed in R (version 4.2.1). The strength of self- and other-blaming emotions experienced by participants were averaged across 27 scenarios in each agency condition. Similarly, we calculated the proportion of trials per agency during which the subjects would most strongly feel a particular emotion and most likely undertake a given action. Such data was used as the dependent variables for permutation-based repeated measures analyses of covariance (ANCOVAs) run using the *aovperm* function from the *permuco* library (Frossand and Renaud, 2021) with 10000 permutations. The models tested the associations of anxiety and its interactions with agency (within-subject condition), controlling for the confounding effects of age and sex. The decision to use a non-parametric approach for the described analyses was guided by the largely non-normal distribution of the emotion- and action-frequency data. Multiple comparison correction was achieved through false discovery rate (FDR < 0.05) applied across each category (i.e. self- vs. other blaming emotions, experienced emotions and undertaken actions).

Additionally, using the original data from the task, where the choices of particular emotions and actions were coded binarily, we ran two types of logistic regression models (*glmer* function from *lme4* library; Bates et al., 2015), similarly to the work of Duan and colleagues (Duan et al., 2021). Firstly, we examined whether apologising, hiding, creating a distance from oneself, and attacking oneself could be predicted by self-blaming emotions (shame, guilt, self-disgust/contempt, and self-indignation) and anxiety, as well as their interactions, controlling for the main effects of age and sex. Secondly, as creating a distance from a friend and attacking them are likely to be motivated by other-blaming emotions (i.e. contempt/disgust towards the friend and indignation/anger towards the friend), we tested such associations using similar models as in the first case, this time putting other-blaming emotions in the place of self-blaming emotions. For the logistic regression analysis, FDR was applied separately for each predictor, taking into account the number of models in which a given variable or interaction term was included.

2.2. fMRI Guilt recollection task

2.2.1. Participants

The guilt recollection task in the functional magnetic resonance imaging (fMRI) setting was performed by 80 individuals, with the majority (N = 71) also forming a part of the MSAT cohort. The composite anxiety scores for the sample were calculated anew, using the same approach as described previously (section 2.1.1.). The characteristics of the cohort are provided in Supplementary Table 1.

2.2.2. Task description

During recruitment for the study, participants were asked to provide 7 instances of memories they felt guilty about and 7 instances of emotionally neutral past events. The choice of personally-relevant situations rather than hypothetical guilt-evoking scenarios was guided by the findings that guilt recollection induces higher activity in the relevant brain circuitry (Mclatchie et al., 2016). To ensure the participants' comfort, the exact details of personal events remained unknown to the experimenters. For each memory, the subjects provided 5 cues, up to 3 words each, that would enable them to identify it afterwards. To make the content of the cues comparable within and across the individuals, we required at least one cue pertaining to the involved people, an associated abstract or concrete object and the location of the event. For both guilt and neutral memories, participants rated how guilty they felt about the particular event

and to what extent they felt they had violated the socially accepted norms of behaviour (Likert scale ranging from 1 (not at all) to 7 (very much)). In the case of the neutral events, to ensure their lack of emotional valence, an additional question was asked probing feelings associated with the particular memory (Likert scale from -3 to 3, i.e. from extremely negative to extremely positive emotions). For the subsequent part of the experiment, 5 memories from each category were chosen. The inclusion criteria were guilt ratings ≥ 4 for the guilt memories, and emotional valence ratings within the -1 to 1 range for the neutral memories.

In the week preceding the fMRI session, the participants filled in a survey pertaining to the chosen stimuli. In some cases the exact wording of the cues was slightly altered by the experimenters for brevity, and so the participants were asked to confirm their ability to correctly identify the memories. They were also prompted to rate how vividly they could relive emotions associated with each event (Likert scale from 1, not vividly at all, to 4, quite vividly). Additionally, three more questions with prespecified answers concerning the type of location (outdoor, indoor, both), number of people involved (0-2, 3-5, > 5), and the time that had passed since each event took place (≤ 1 year, 2-5 years, > 5 years) were asked, with the associated information serving as a part of the task performed in the scanner, enabling us to test whether the correct memory was retrieved.

Prior to entering the scanner, the participants were familiarised with the task procedure. To avoid any repetition suppression effects, the stimuli presented during the familiarisation run were different from the participant-specific memories. The guilt recollection task was administered with PsychoPy (version 2022.2.5; Peirce et al., 2019), and was presented to the participants using MRI-compatible goggles (VisuaStim Digital, Resonance Technology Inc.). The behavioural responses were recorded with the right-hand device from the MRI-compatible four-key button box set.

The schematic representation of the guilt recollection task is presented in Figure 1. Each trial began with a 10 s period during which cues related to specific memories were presented. The participants were instructed to ‘relive’ the associated emotions upon recognising the event. In the subsequent stage, the subjects would have 4 s to answer a question regarding the location, socialness or age of the memory. At the end of each trial, the participants performed from 3 to 5 repetitions of a simple magnitude judgment task. Participants had to choose which of the two numbers presented at the bottom of the screen was closer to the target number presented above. The number of arithmetic task repetitions was counterbalanced across the run.

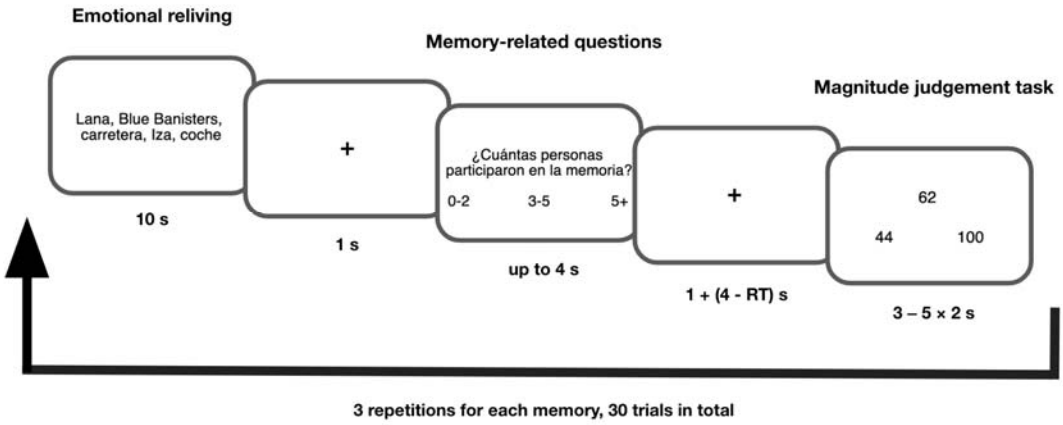

Figure 1. Schematic representation of the guilt recollection task. Abbreviations: RT, reaction time.

We included the memory-related questions and the magnitude judgement task to shift attention of participants from internally- to externally-focused cognition, reducing activity in the socio-emotional brain circuitry before the next trial. The magnitude judgement tasks also served as a non-semantic baseline for the imaging contrast (Binney et al., 2016). For a similar purpose, the guilt and neutral memories were presented in a pseudo-randomised order with not more than two examples of the same condition presented consecutively. All the memories appeared 3 times, each time followed by a question concerning a different aspect of the event, yielding 30 trials in total (13 min).

After the scanning session, participants were asked whether they could relive emotions associated with each memory upon all the repetitions and how vivid the experience had been. In the case of difficulties performing the task, the indicated trials were excluded from the neuroimaging analyses. Additionally, the approach-avoidance motivation related to each event was measured by inquiring whether the participants felt like distancing themselves from the involved people, objects and places, or approaching them (Likert scale, ranging from -3 to 3).

2.2.4. MRI data acquisition

Neuroimaging data was collected with a 3T General Electrics SIGNA Architect scanner. For high-resolution structural images, T1 MP-RAGE sequence was used. The functional T2*-weighted data was collected with a multiband gradient echo-planar imaging sequence (50 axial slices collected in the interleaved order; 2.5 mm isotropic voxel; repetition time = 2 s; echo time = 20.4 ms; flip angle = 90°; multiband acceleration factor = 2; left-right phase-encoding direction). To account for the non-steady state of the magnetic field, 10 volumes were added at the beginning of the sequence, yielding the total scanning time of 13 min 20 s. The decision to use the left-right vs. anterior-posterior phase-encoding direction for the task sequence was guided by higher temporal signal-to-noise ratio (tSNR) observed in the brain areas of interest during the piloting stage, in line with the previous findings suggesting that phase encoding direction matters (Cao et al., 2023; Wang et al., 2023; Halai et al., 2014).

2.2.5. MRI data analysis and seed delineation

Preprocessing of the data was conducted using AFNI (Cox, 1996) and FSL (Jenkinson et al., 2012) packages. The decision to use a custom pipeline for the task fMRI data, as compared to the more standardised approach of fMRIprep (Esteban et al., 2019), was guided by suboptimal performance of the latter tool for distortion correction of the images acquired with the current T2*-weighted sequence (i.e. left-right phase-encoding).

Anatomical images were skull-stripped, warped to the MNI space, and segmented to obtain individual cerebrospinal fluid (CSF) masks. The preprocessing of the task data began with deleting the first 5 volumes to allow for signal equilibration. Subsequently, the matrix for motion correction was obtained, and the data was despiked. Then, matrices for susceptibility distortion correction (derived using two separate acquisitions with the opposite phase-encoding directions) and co-registration to the anatomical image were calculated. The spatial transformation of the functional data was done in one step, combining the matrices for motion and distortion correction, coregistration and normalisation to the MNI space.

Following smoothing with a 5 mm Gaussian kernel, the subject-level analysis was performed. The models were run with the pre-whitening option to account for temporal autocorrelations in the data. The nuisance regression included: motion censoring (with a separate regressor for each volume with ≥ 0.5 mm framewise displacement), 12 motion parameters (6 demeaned originals and their first-order derivatives), the CSF time course (physiological noise), and 6 polynomials (low-frequency drifts; determined with the "1 + int(D/150)" equation, where D is the sequence duration in s). The brain activity during each part of the paradigm, i.e. emotional reliving, answering the memory-related questions and magnitude judgement task, was modeled separately by convolving box-car responses with the canonical hemodynamic response function (HRF). The individual brain activity maps for the contrast of interest were generated by subtracting activation patterns associated with the emotional reliving of the guilt and neutral memories for the full epoch length, i.e. 10 s.

Two seeds were chosen for the psychophysiological interactions (PPI) analysis. The left (MNI: −50, 4, −10) and right sATL (MNI: 57, −3, −6) were defined as spheres with a 6 mm radius (Green et al., 2012) centered at the peak coordinates from previous neuroimaging studies on guilt processing (Green et al., 2012; Gifuni et al., 2017; Zareba et al., 2024a). The PPI analyses excluded motion censoring to avoid time series discontinuity. To create PPI regressors, mean time courses of seeds were extracted from the residual files of the recalculated task activity-related regression, resulting in the physiological regressors. Following deconvolution, PPI interaction terms were calculated by multiplying the time courses of neural activity with those of psychological task manipulations (i.e. reliving guilt vs. neutral memories) and reconvolving them with HRF. To generate whole-brain maps for the task-dependent connectivity effects, the subject-level analyses were rerun, this time including the physiological and PPI terms.

2.2.6. Group-level analysis

2.2.6.1. Behavioural data

For all participants, we calculated separately for guilt and neutral memories the mean values for the following measurements: the associated feelings of guilt, perceived social code violation, vividness of the recall before and during the scanning session, approach-avoidance motivation, salience, as well as accuracy and mean reaction times (RTs) for the questions pertaining to the memory whereabouts. Salience of individual memories was defined as the absolute value of the reported approach-avoidance. Additionally, we calculated the number of times participants could

successfully relive in the scanner each memory type. For all of the aforementioned variables, permutation-based repeated measures ANCOVAs were run using the R's *aovperm* function from the *permuco* library (Frossand and Renaud, 2021) with 10000 permutations. The models tested the associations with anxiety and its interactions with memory type (within-subject condition), controlling for the confounding effects of age and sex. The same approach was used for testing the differences of vividness across each memory type before and during the task execution. To analyse the associations of anxiety with mean emotional valence of neutral memories, as well as well as accuracy and mean RTs for the magnitude judgement task, permutation-based linear regression models were run with the *lmperm* function of the *permuco* library (Frossand and Renaud, 2021) using 10000 permutations. Data of one and three participants was excluded from the analysis of accuracy and mean RTs for, respectively, the memory- and arithmetics-related parts of the task due to the use of incorrect response buttons.

2.2.6.2. Neuroimaging data

The whole-brain analysis of neuroimaging data was performed in AFNI. To identify patterns of brain activity and sATL task-dependent connectivity consistently associated with reliving of guilt vs. neutral memories across the cohort, one sample t-tests were run using *3dttest++*. In turn, associations with anxiety were tested using *3dMVM* models (Chen et al., 2014), with age and sex controlled as covariates. Cluster-level family wise error-rate correction (FWE < 0.05) with voxel-level thresholding at $p < 0.001$ was used for significance testing.

Furthermore, a region-of-interest (ROI) approach was used to investigate the functioning of the sATL - sgACC circuitry in detail. The left and right sATL ROIs were defined as previously described (section 2.2.5), while the bilateral sgACC ROI was set as a 6 mm radius sphere centered at the x = 0, y = 15, z = -5 MNI coordinates (Moll et al., 2006; Zareba et al., 2024a). The mean brain activity of all voxels within each of the three areas, as well as PPI of the left and right sATL with sgACC were used as dependent variables. The linear regression models were run with R's *lm* function, testing for associations with anxiety and keeping age and sex as covariates. FDR was applied to correct for multiple comparisons.

2.2.6.3. Associations of brain activity with molecular architecture of neuromodulatory systems

To confirm that the NE, 5-HT and DA systems were involved in guilt processing in our sample, we used publicly available atlases to delineate bilateral locus coeruleus, dorsal raphe and ventral tegmental area in the MNI space (Betts et al., 2017; Beliveau et al., 2015; Murty et al., 2014; see Supplementary Figure 1). The process is described in more detail elsewhere (Zareba et al., 2024b). The average ROI-wise values were extracted in each participant from the brain activity contrast map for the reliving of guilt vs. neutral memories. Subsequently, FDR-corrected one sample t-tests were calculated. The analysis indicated increased activity of all three neuromodulatory brain regions during guilt processing (Supplementary Figure 2), warranting the procedures described below. This confirmatory analysis was not performed for the oxytocin system as the hypothalamic oxytocinergic nuclei could not be properly delineated using the current imaging sequence.

The gold standard for testing differential regional associations of brain activity with the amount of transporters and receptors would be collecting both types of data in the same set of participants. Nevertheless, acquisition of such data, for example using positron emission tomography (PET), is costly and requires advanced infrastructure, often unavailable to research centers. The use of normative maps of receptor and transporter distributions, however, opens up the possibility of making preliminary inferences on such associations by performing cross-modality correlations of group-averaged voxel-level values.

Therefore, utilising such an approach, we first created a binary mask of regions with significantly higher and lower brain activity associated with guilt processing in our study on the group level, and subsequently used the atlases of cortical, subcortical and cerebellar regions (Fan et al., 2016; Diedrichsen et al., 2009) for parcellation. As a means of striking a balance between spatial resolution and power to detect meaningful effects within a region, we ensured that each of the parcels contained at least 40 voxels. In the cases when original atlas-based regions contained a smaller number of voxels surviving the cluster-level FWE thresholding, we merged such areas into larger clusters based on the visual convergence of their connectivity patterns and associated cognitive functions, as provided in the atlas (Fan et al., 2016; see Supplementary Table 2 and Data availability section). For instance, all the unilateral subdivisions of the postcentral gyrus were put together to form one region.

With the use of Neuromaps (Hansen et al., 2022), we obtained normative PET maps for:

- dopamine transporter (DAT), as well as D_1 and D_2 receptors (Dukart et al., 2018; Kaller et al., 2017; Smith et al., 2019; Sandiego et al., 2015; Zakiniaeiz et al., 2019; Slifstein et al., 2015; Sandiego et al., 2019)
- serotonin transporter (5-HTT) as well as 5-HT_{1B}, 5-HT_{2A}, 5-HT_4 and 5-HT_6 receptors (Beliveau et al., 2017; Gallezot et al., 2010; Murrough et al., 2011a; Murrough et al., 2011b; Matuskey et al., 2014; Pittenger et al., 2016; Saricicek et al., 2015; Baldassarri et al., 2020; Radhakrishnan et al., 2018; Radhakrishnan et al., 2020; Savli et al., 2012)
- norepinephrine transporter (NET; Ding et al., 2010; Li et al., 2014; Sanchez-Rangel et al., 2020; Belfort-DeAguiar et al., 2018)

As there are no known PET tracers for oxytocin receptors (OXTR), we used the maps of predicted mRNA expression from post-mortem brains (Gryglewski et al., 2018). All the maps of neuromodulatory systems were resampled to the task fMRI data resolution, followed by voxel-wise z-score normalisation. For each ROI, we first extracted for all the voxels (group-level) t-stats from the contrast map of interest and Z-scores from the external maps of neuromodulatory molecules densities, and subsequently used Spearman correlations to probe the cross-modality associations. FDR (< 0.05) was used to correct for the number of regions (N = 100), separately for each molecular map.

2.3. Resting-state fMRI correlates of self-blaming behaviour

2.3.1. Participants

A subset of participants (N = 86) who performed the MSAT task additionally underwent scanning with a resting-state fMRI paradigm. Following the methodology from the previous experiments, we recalculated the composite anxiety scores for the subsample. The more detailed characteristics of the group can be found in Supplementary Table 3.

2.3.2. MRI data acquisition and analysis

Neuroimaging data was collected using the same parameters as previously described in the section 2.2.4., the only differences for the functional sequence being the use of standard anterior-posterior phase-encoding direction and acquisition of 185 volumes (6 min 10 s). The resting-state data was always acquired between the anatomical and task sequences to avoid the latter's confounding influence (Li et al., 2016). During the scan, the participants were instructed to keep their eyes open and focused on a black fixation cross on the white background.

The data was preprocessed with fMRIprep version 23.2.1. (Esteban et al., 2018), based on Nipype 1.8. (Gorgolewski et al., 2011). In summary, the T1-weighted image was corrected for intensity non-uniformity, skull-stripped, segmented and normalised to the MNI space. The

resting-state data was motion, fieldmap and slice-timing corrected, followed by coregistration to the anatomical image and normalisation. To allow for signal equilibration, the first 5 volumes of the functional run were discarded. Such fMRI data was then processed with AFNI (Cox, 1996), where it was smoothed with a 5 mm Gaussian kernel, followed by detrending, denoising and band-pass filtering (0.01-0.1 Hz frequency range), all applied in one step. The nuisance regressors included the mean CSF and white matter time courses, the original 6 motion parameters and their first-order derivatives. In the case of the fractional amplitude of low frequency fluctuations (fALFF) calculations, the polynomial detrending was not applied, following recent guidelines (Woletz et al., 2019).

Four types of measurements were derived from the data. Firstly, to probe the magnitude of resting-state activity, ALFF and fALFF were calculated. ALFF was defined as the absolute signal power within the 0.01-0.1 Hz frequency range, while fALFF was calculated as the ratio of ALFF to the total signal power across the entire frequency spectrum. While ALFF has higher test-retest reliability (Zuo et al., 2010), fALFF is more independent from the physiological noise (Zou et al., 2008), rendering the two approaches complementary. Both metrics were mean-normalised within each subject prior to the group analysis.

Secondly, to assess the resting-state functional connectivity within the circuitry of interest, two additional types of measures were calculated. To study the coupling of sATL in detail, we averaged the time courses of the low frequency blood-oxygen-level-dependent (BOLD) signal in the left and right hemisphere ROIs separately, correlated them with the time series of all the other voxels in the brain, and normalised the distribution of the resulting Pearson correlation coefficients using Fisher's z transform. In turn, to obtain the information on how all the brain regions associated with guilt processing were generally integrated within the relevant circuitry, we first masked each participant's preprocessed image using the results from the guilt reliving-related one sample t-test, and subsequently calculated global connectivity, i.e. the average correlation coefficient of each voxel's time series with the rest of the included brain areas.

2.3.3. Group-level analysis

The voxel-level analyses for the previously described neural measures were performed using AFNI's *3dMVM* (Chen et al., 2014). As explained before, in the MSAT participants rated self-blaming emotions (Likert scale 1 to 7) of hypothetical scenarios in which they (self-agency) or their friend (other-agency) were behaving counter to social and moral values. The neuroimaging models investigated associations with the agency-averaged self-blaming emotions, controlling for age and sex. Cluster-level family wise error-rate correction (FWE < 0.05) with voxel-level thresholding at $p < 0.001$ was used for significance testing. For significant results, we extracted the mean values of the tested metrics inside each cluster, and subsequently correlated them with the composite anxiety scores.

Furthermore, similarly to the task-based analysis, we used the ROI approach to probe the functioning of sATL in detail. The left and right sATL ROIs were defined as previously explained in the section 2.2.5, and their mean ALFF, fALFF and global connectivity values were extracted. The associations with self-blaming emotions and anxiety scores were tested using separate linear regression models (R's *lm* function), controlling for the effects of age and sex. Multiple comparison correction was achieved using FDR. The decision not to include the bilateral sgACC in the analyses was guided by the relatively lower tSNR observed in this area with the resting-state sequence, as compared with the task-related data acquired with the left-right phase encoding direction.

3. Results

3.1. Higher anxiety is linked to self-blaming and hiding biases, and more self-centered perspective when feeling negative emotions about oneself

The first set of analyses (described in section 2.1.3) tested in the full sample of 140 subjects whether self-blaming emotions and action tendencies measured in the MSAT task differed depending on individual anxiety levels. The results confirmed the self-blaming bias of highly anxious individuals ($F = 22.02$, $p_{FDR} < 0.001$; Figure 2A), which was paralleled by only nominally significant association with a higher prevalence of the guilt feelings ($F = 5.85$, $p_{uncorr.} = 0.016$, $p_{FDR} = 0.114$; Supplementary Figure 3A). As for the action tendencies, the repeated measures ANCOVA additionally linked elevated anxiety levels with more self-attacking behaviours ($F = 7.23$, $p_{FDR} = 0.046$; Figure 2B).

The logistic regression analysis complemented the last result by demonstrating, irrespective of the experienced emotions, higher likelihood of hiding in the more anxious participants ($\beta = 0.24$, standard error (SE) = 0.08, $p_{FDR} = 0.029$; Figure 2C), corroborating the trend-level association obtained using the former approach ($F = 4.33$; $p_{uncorr.} = 0.036$; $p_{FDR} = 0.085$; Supplementary Figure 3C). Importantly, logistic regression enabled us to link individual levels of anxiety with specific patterns of behaviour. Namely, highly anxious participants were less likely to create distance from themselves when experiencing shame ($\beta = -0.61$, SE = 0.18, $p_{FDR} = 0.002$; Figure 2D) or self-anger ($\beta = -0.63$, SE = 0.19, $p_{FDR} = 0.003$; Figure 2E). As such, the current results confirm the self-blaming bias of subclinically anxious individuals (Cândea and Szentagotai-Tătar, 2018), linking it with similar maladaptive action tendencies as those observed in MDD patients (Duan et al., 2021; Duan et al., 2023).

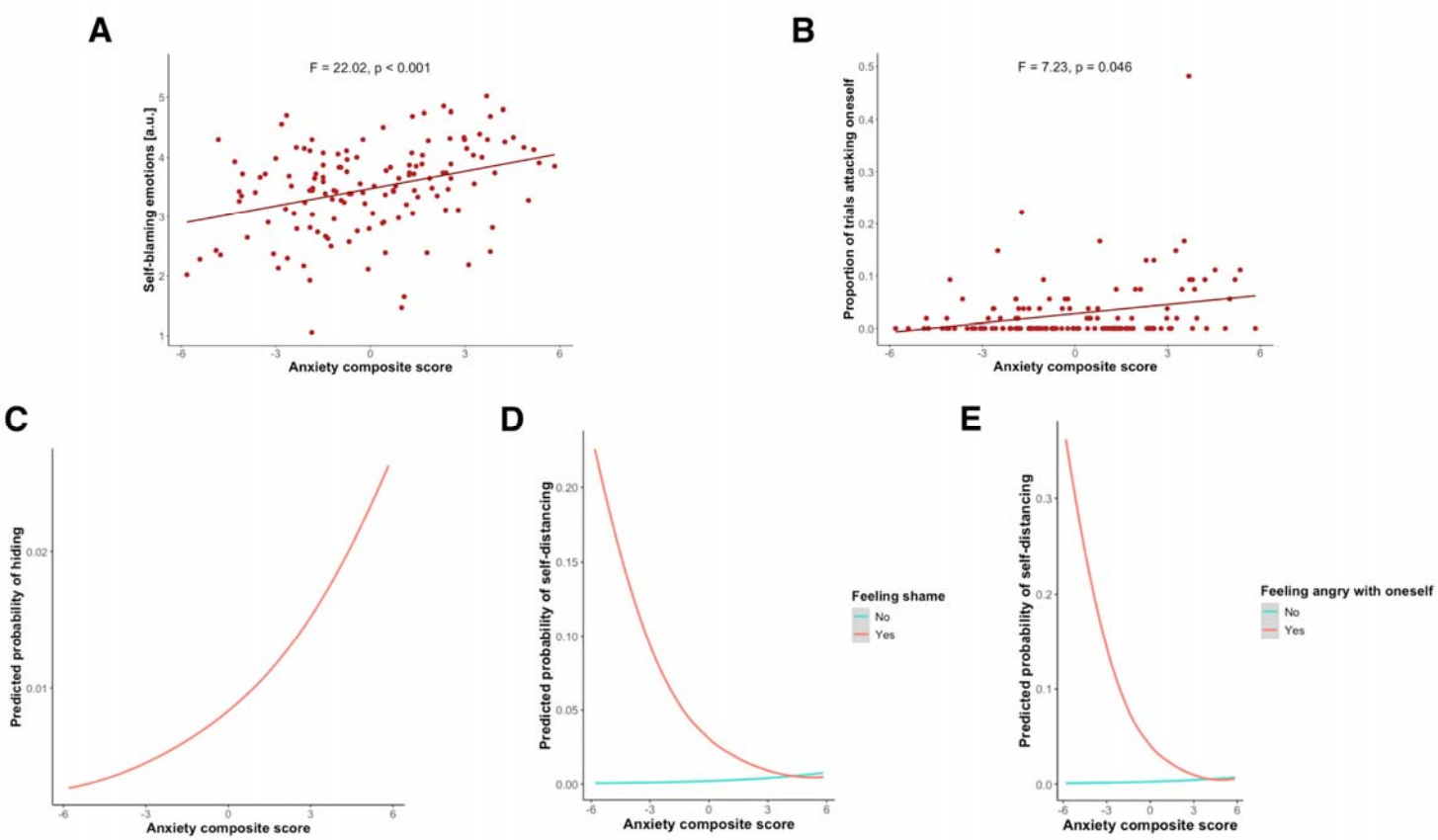

Figure 2. Associations of anxiety levels with self-blaming emotions and action tendencies from the Moral Sentiment and Action Tendencies Task (MSAT). Higher anxiety was related to elevated (A) self-blaming emotions, (B) self-attacking behaviour and (C) probability of hiding, regardless of experienced emotions. When feeling negative emotions towards oneself, such as (D) shame or (E) anger, highly anxious individuals were also less likely to create a distance from themselves.

The remaining trend-level associations with anxiety can be found in the Supplementary Figure 3, while the findings for agency and sex are demonstrated in Supplementary Figures 4-6.

3.2. Subclinical anxiety facilitates emotional reliving but is unrelated to the approach-avoidance motivation or salience of the guilt memories

The second set of analyses (section 2.2.6.1) was focused on the behavioural data associated with the fMRI guilt recollection task. As expected, guilt memories were characterised by higher subjective guilt ratings ($F = 5497.89$; $p < 0.001$), perceived social code violation ($F = 280.86$; $p < 0.001$) and salience ($F = 74.88$, $p < 0.001$), as well as less approach/more avoidant motivation ($F = 13.28$, $p < 0.001$) compared to the neutral events (Supplementary Table 4; Supplementary Figure 7). While there were no differences in the vividness of the two types of memories when recalled before ($F = 0.84$, $p = 0.358$) or during the scanning session ($F = 0.32$, $p = 0.578$), both were characterised by lower ratings during scanning ($F = 54.97$ and $F = 19.15$ for, respectively, guilt and neutral memories, both $p < 0.001$). The vividness ratings nonetheless remained at satisfactorily high level (3.09 ± 0.46 for guilt memories, 3.14 ± 0.75 for neutral memories, with 4 as the maximum score), confirming that participants could properly relive the associated emotions in both contexts.

The participants were also less accurate ($F = 49.45$, $p < 0.001$) and slower ($F = 56.47$; $p < 0.001$) when responding to the questions probing whereabouts of the guilt memories, suggestive of increased cognitive engagement as compared to the neutral past events, which is further corroborated by the reports of more difficulty reliving the associated guilt emotions ($F = 5.35$; $p = 0.021$). Interestingly, individual anxiety levels positively predicted one's ability to relive the emotions, regardless of the memory type ($F = 4.90$, $p = 0.031$; Supplementary Figure 8A). In contrast with the hypothesis, however, anxiety was unrelated to the approach-avoidance motivation and salience of the memories (Supplementary Table 4). Therefore, given the widespread and normal distribution of these two measures (Supplementary Figure 7), they were treated as additional between-subject factors of interest for an exploratory analysis of the task neuroimaging data.

The full results of the previously described analyses can be found in Supplementary Table 4. Supplementary Figure 7 demonstrates the observed differences between the guilt and neutral memories, while Supplementary Figure 8B-F depicts associations of their characteristics with sex and age.

3.3. Anxiety, approach-avoidance motivation and self-blaming tendency are related to largely distinct activity and connectivity patterns within the anterior temporal lobe circuitry

Emotional reliving of guilt, as compared to neutral, memories was associated with increased activity in a widespread network consisting of medial and ventrolateral frontal cortices, anterior and posterior temporal lobes, precuneus, insula, striatum, amygdala, hippocampus, thalamus and cerebellum (Supplementary Figure 9). Despite the involvement of bilateral regions, the activation pattern was visibly left-lateralised, which corroborates the previous meta-analytic evidence (Gifuni et al., 2017). In the entire sample, guilt processing was also related to higher task-related functional connectivity between the right sATL and the left superior frontal gyrus (T

= 4.79, k = 31, MNI: -8, 30, 50; Supplementary Figure 10). No such findings were observed for the coupling of the left sATL.

The whole-brain models for guilt-related activity revealed no significant associations with the composite anxiety scores, approach-avoidance towards the guilt memories or their salience. In turn, the ROI-level analysis revealed higher activity of the left sATL in individuals with greater approach motivation towards their guilt memories (T = 2.69, p_{FDR} = 0.027). No such links were found for either the bilateral sgACC (T = -1.28, $p_{uncorr.}$ = 0.203) or the right sATL (T = -0.73, $p_{uncorr.}$ = 0.469). Similarly, anxiety and salience were unrelated to the activity of the bilateral sgACC (anxiety: T = -1.86, $p_{uncorr.}$ = 0.067; salience: T = -1.16, $p_{uncorr.}$ = 0.251), left sATL (anxiety: T = -1.39, $p_{uncorr.}$ = 0.168; salience: T = 1.28, $p_{uncorr.}$ = 0.204) or right sATL (anxiety: T = -0.84, $p_{uncorr.}$ = 0.402; salience: T = 1.37 , $p_{uncorr.}$ = 0.175).

As for the task connectivity, the whole-brain analyses revealed significant findings only for the approach-avoidance domain where increased aversion towards one's guilt memories was positively associated with the right sATL's coupling with ipsilateral paracentral (F = 23.89, k = 43, MNI: 12, -38, 52) and inferior parietal lobules (F = 18.66, k = 27, MNI: 32, -56, 32). In turn, the ROI-level analysis confirmed our hypothesis of increased task-dependent functional connectivity between the left sATL and bilateral sgACC in highly anxious individuals (T = 2.54, p_{FDR} = 0.026), while no such associations were found for the right sATL (T = -0.52, $p_{uncorr.}$ = 0.604). Furthermore, the connectivity between the sATL and bilateral sgACC was unrelated to either approach-avoidance towards guilt memories (left sATL: T = 0.46, $p_{uncorr.}$ = 0.649; right sATL: T = 1.49, $p_{uncorr.}$ = 0.141) or their salience (left sATL: T = 0.07, $p_{uncorr.}$ = 0.947; right sATL: T = -0.89, $p_{uncorr.}$ = 0.379).

Given the associations of anxiety with the outcomes of the MSAT task (section 3.1.), we subsequently investigated whether the increased task-dependent functional connectivity between the left sATL and bilateral sgACC found in highly anxious individuals was similarly linked to the strength of self-blaming emotions and highlighted behavioural patterns using the overlapping sample across the two experiments (N = 71). We followed the same methodology as previously (section 2.1.3), with the exception of testing only the influence of guilt in the logistic regression models. A trend-level interaction emerged in which higher task-dependent functional connectivity between the temporal and frontal areas was related to lower probability of hiding when one was feeling guilt (β = -0.82, SE = 0.37, p_{FDR} = 0.051; Supplementary Figure 11). Therefore, despite anxious individuals demonstrating a higher probability of socially avoidant behaviours, a guilt-dependent connectivity pattern associated with elevated anxiety was inversely linked to hiding, which stays in contrast with the expected similarity of the effects, indicating complex associations of behaviour with emotion-specific neural patterns within the studied circuitry. Of note, the discussed task connectivity pattern was unrelated to the strength of self-blaming emotions (r = 0.11, $p_{uncorr.}$ = 0.353), the frequency of self-attacking behaviours (ρ = -0.06, $p_{uncorr.}$ = 0.628) or the probability of self-distancing when feeling guilt (β = 0.14, SE = 0.56, $p_{uncorr.}$ = 0.802).

Last but not least, the analysis of the resting-state data indicated that higher resting-state activity (ALFF) in the right temporal pole was related to less pronounced self-blaming emotions (F = 26.10, k = 15, MNI: 30, 14, -36). Surprisingly, however, this neural pattern was not related to the composite anxiety scores (r = -0.02, $p_{uncorr.}$ = 0.882). The remaining whole-brain models revealed no significant findings for fALFF, global connectivity within the circuitry or the seed-based coupling of the left and right sATL. The ROI-level analysis similarly demonstrated that neither self-blaming emotions, nor the composite anxiety scores were associated with the sATL's ALFF, fALFF or global connectivity (Supplementary Table 5).

All the significant neuroimaging results across the previously described analyses are summarised in Table 2 and Figure 3. No associations with age or sex were found.

Table 2. Significant associations of activity and connectivity within the bilateral polar and anterior temporal lobe circuitry with anxiety, approach-avoidance motivation towards one's guilt memories and self-blaming emotions. For guilt-dependent functional connectivity results, the first area represents the seed region.

Neural measure	Brain region	MNI coordinates	Voxels	Statistics
Anxiety				
Guilt-dependent functional connectivity	L superior anterior temporal lobe B subgenual anterior cingulate cortex	-50, 4, -10 0, 15, −5	61 61	T = 2.54 [R]
Approach-avoidance motivation				
Guilt processing-related activity	L superior anterior temporal lobe	-50, 4, -10	61	T = 2.69 [R]
Guilt-dependent functional connectivity	R superior anterior temporal lobe R paracentral lobule	57, -3, -6 12, -38, 52	55 43	F = 23.89 [W, neg.]
Guilt-dependent functional connectivity	R superior anterior temporal lobe R inferior parietal lobule	57, -3, -6 32, -56, 32	55 27	F = 18.66 [W, neg.]
Self-blaming emotions				
Resting-state ALFF	R temporal pole	30, 14, -36	15	F = 26.10 [W, neg.]

Abbreviations: L, left; R, right; B, bilateral; ALFF, amplitude of low frequency fluctuations.
[R] Region-of-interest analysis.
[W] Whole-brain analysis.
[neg.] Negative link with the reported psychological measure or an association with more avoidant motivation.

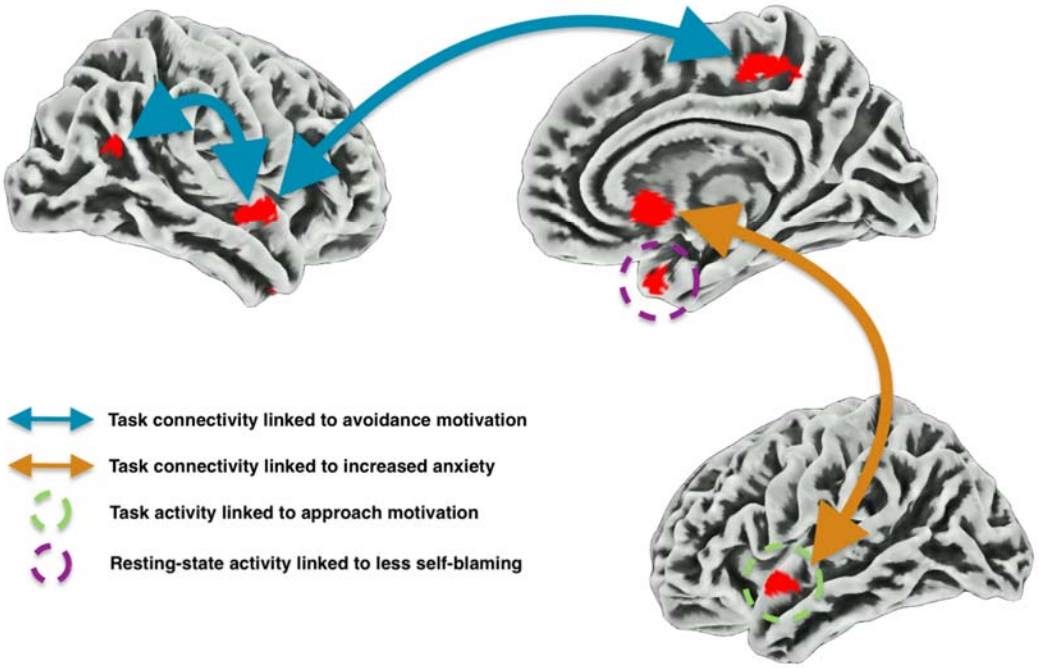

Figure 3. Associations of the connectivity and activity of the polar and anterior temporal regions with subclinical anxiety, approach-avoidance motivation and self-blaming. The results pertaining to the avoidance motivation and self-blaming survived the cluster-level family-wise error thresholding ($p_{FWE} < 0.05$), whereas the links with anxiety and approach motivation were thresholded at the region-of-interest level using the false discovery rate correction ($p_{FDR} < 0.05$)

3.4. Neuromodulatory systems may differentially shape guilt-related activity across the relevant brain networks

The last set of analyses (described in section 2.2.6.3.) aimed to assess the potential influence of neuromodulatory brain systems on guilt-related activity in our sample. To achieve that goal, we used external normative (population-averaged) maps of their transporter and receptor densities, and correlated them with group-averaged measures of task-evoked activity in our study. The analyses revealed robust associations for all the tested neuromodulatory systems, i.e. 5-HT, DA, NE and OXT, indicating that the discussed neurotransmitters might play a crucial role in shaping the neural dynamics when one experiences strong and negative self-referential emotions (Figure 4). Non-thresholded and thresholded correlation maps for specific molecules are available on the NeuroVault platform (see Data availability section).

Interestingly, the results hint at a possibility of differential involvement of specific neurotransmitters across the brain, even if the areas form part of a tightly cooperating network. For instance, the activity in the right-sided dorsolateral prefrontal cortex and anterior inferior parietal lobule, mapping onto the lateral frontoparietal control network, crucial for voluntary emotion regulation (Morawetz et al., 2020), was correlated with indices of all 4 neuromodulatory systems, while the link with NE was absent for the more posterior parts of the inferior parietal lobule. Similarly, the activity in the bilateral hippocampi and amygdalae, key regions for emotional memory, was associated solely with 5-HT and OXT molecules density, while the insula, another region strongly implicated in emotion processing and etiology of mood and anxiety disorders (Picó-Pérez et al., 2017; Zareba et al., 2024a; Zareba et al., 2025), displayed a more complex, subregion-specific pattern.

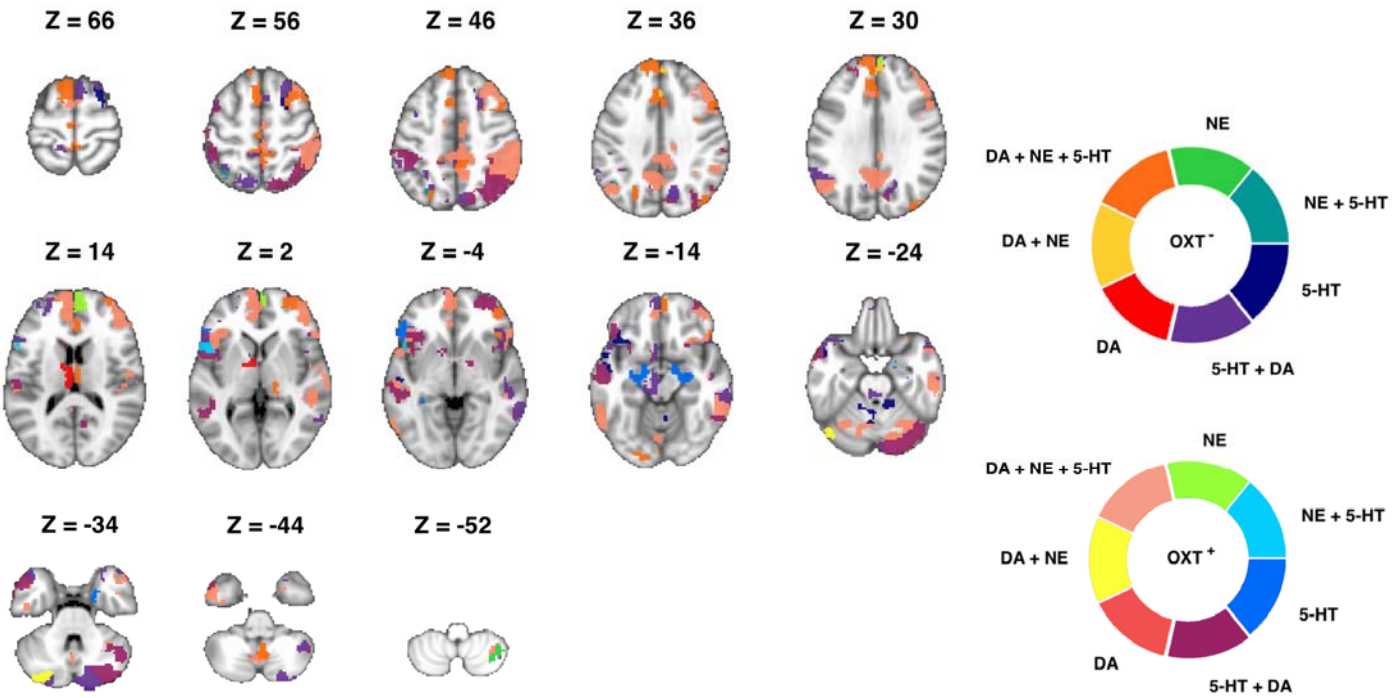

Figure 4. Summary of the regional associations between guilt-related brain activity in our sample and the amounts of neuromodulatory receptors and transporters derived from external normative maps. OXT^+ and OXT^- stand for, respectively, the presence or lack of associations with the oxytocinergic system. Abbreviations: DA, dopamine; NE, norepinephrine; 5-HT, serotonin.

Discussion

The results of the current study confirm the self-blaming bias in subclinically anxious individuals, linking it with more pronounced self-attacking and socially avoidant behaviours. Importantly for understanding the aetiology of maladaptive emotion regulation, when experiencing negative emotions about themselves, such as shame and self-anger, highly anxious individuals were less likely to disengage from self-focused thoughts. On the neural level, these findings were paralleled by increased guilt-dependent functional connectivity between the left sATL and bilateral sgACC in the more anxious participants, and lower amplitude of resting-state activity in the right temporal pole in subjects with more pronounced self-blaming emotions. Interestingly, despite higher proneness to social avoidance observed across a variety of hypothetical social scenarios in the MSAT task, individual anxiety levels were unrelated to approach-avoidance motivation pertaining to the guilt memories. This aspect of the guilt experiences was nevertheless similarly linked to the sATL circuitry, with higher task activity in the left sATL linked to more approach motivation, and higher guilt-dependent right sATL connectivity with ipsilateral paracentral and inferior parietal lobules linked to more avoidant feelings. Last but not least, the analyses performed with the normative maps of molecular markers of DA, NE, 5-HT and OXT systems indicated that each of them may differentially shape guilt-related activity across the relevant brain networks, potentially increasing our understanding of how alterations in their neurotransmission strength could contribute to guilt symptomatology.

The presented findings on the self-blaming emotions and associated action tendencies are largely in line with the study's hypotheses. Nevertheless, despite the crucial role played by the

sense of agency in the formers' development (Caspar et al., 2020), we did not observe the modulating effect of the agency condition on the associations between anxiety and outcomes of the MSAT task, which stood in contrast with our expectations. This result points towards the accounts of overgeneralisation of guilt in subclinically anxious individuals (Cândea and Szentagotai-Tătar, 2018), which could be potentially explained by their increased sense of responsibility for the actions of others (Apetroaia et al., 2015). Importantly, the behavioural patterns identified in the current work are well positioned to explain the symptomatology observed in highly anxious people. The avoidance bias may lead to social withdrawal and isolation, decreasing the likelihood of rewarding social interactions (Silk et al., 2012), and together with self-attacking behaviours could reinforce the lower self-esteem typically observed in that group (Fernandes et al., 2022). Moreover, the inability to disengage from self-centered thoughts when feeling negative emotions about oneself might give rise to rumination. Such increased understanding of the self-blaming biases of subclinically anxious individuals might therefore prove informative for clinical psychologists and psychotherapeutic efforts.

Interestingly, in the fMRI task, we observed that highly anxious participants reported greater success at reliving the emotional aspects of memories independently of the memory type (guilt vs. neutral), which does not fully align with the typical accounts of their enhanced encoding of negatively valenced episodic memories, with either intact or diminished encoding of neutral events (Zlomuzica et al., 2014). However, a recent work demonstrated that elevated anxiety levels are linked to a particularly salient negative mode of episodic memory retrieval, which might create a downstream bias in encoding and subsequent retrieval of otherwise neutral information (Lee and Fernandes, 2017). While the effect was observed across the timescale of minutes, the neutral memories in the current work typically spanned across a week preceding the scanning session. As such, our results suggest that similar processes might also be relevant for episodic memory retrieval on longer, more intermediate timescales. Last but not least, although we hypothesised that higher anxiety levels would be related to increased salience or avoidance towards the guilt memories, we did not observe such associations. This comes as a surprise, given the fact that we observed an avoidance bias in the MSAT task, but could be potentially explained by the inclusion of a limited number of memories uniformly associated with strong feelings of guilt, which may similarly affect anxious and non-anxious individuals, unlike the broader range of social scenarios tested in the first study.

The current study also provides important insights into the alterations within the guilt processing circuitry that might contribute to these behavioural observations. Confirming our hypothesis, we observed increased guilt-dependent functional connectivity between the left sATL and bilateral sgACC. This corroborates our previous finding linking the increased functional interconnectedness of the left sATL within the guilt processing network with more pronounced self-blaming behaviours (Zareba et al., 2024a). The left sATL has been linked to the integration of social and emotional information into semantic knowledge and therefore could be a key region for representing concepts like *guilt* (Binney et al., 2016). This integration could be facilitated via the uncinate fasciculus, a white matter tract which connects the ATL with medial prefrontal regions that include the posterior sgACC (Sakata et al., 2019) and process cues pertaining to self-worth and social affiliation (Will et al., 2017; Zahn, 2025). Therefore, we interpret the increased task-dependent functional connectivity between the two areas as a potential marker of stronger contribution of guilt experiences and their associated meaning to the neural computations performed in sgACC, which may lead to the feelings of worthlessness and social difficulties observed in anxious individuals (Will et al., 2017; Fernandes et al., 2022). Importantly, similar findings have been reported in MDD patients, albeit for the right sATL, where this neural signature is believed to reflect a fully remitting form of the disorder with higher risk of recurrence but also better chance of remission (Lythe et al., 2015; Fennema et al., 2023; Zahn, 2025).

In the case of our study, the right hemispheric contributions to self-blaming emotions were observed in the form of the negative link with the amplitude of resting-state activity in the temporal pole, an adjacent area that connects social processing with affective cognition (Lambon Ralph et al., 2017). Individuals with negative emotional biases tend to overgeneralise information related to self-blame and self-criticism (Beck, 1963), a process that was linked to functional disconnection of the right sATL in MDD patients (Green et al., 2013). A body of work suggests, however, that the polar temporal region might also contribute to these observations. Increased activity within this area in females subjected to sexual objectification comments was positively linked to self-esteem and negatively associated with shame proneness (Monachesi et al., 2024), while larger grey matter volumes were related to seeking and enjoying social relationships (Lebreton et al., 2009), a behaviour that is inextricably linked to self-worth (Harris and Orth, 2020). Our result of increased temporal pole ALFF being related to lower self-blaming is therefore in line with the above account. While an important methodological distinction comes in the fact that in the current study this association was observed during task-free resting-state conditions, during this period individuals typically engage in retrospective memories or prospective thoughts (Delamillieure et al., 2010), which quite likely requires social semantic and affective processing. Surprisingly, the discussed neural pattern was unrelated to individual anxiety levels, which nevertheless parallels our previous report of only partially overlapping neural correlates between these two phenomena (Zareba et al., 2024a). Similarly, the results stemming from this work and previous studies appear to suggest differential involvement of the right vs. left sATL in self-blaming symptomatology observed in MDD and subclinical anxiety (Green et al., 2012; Green et al., 2013; Lythe et al., 2015; Zahn et al., 2019; Jaeckle et al., 2023; Fennema et al., 2023; Zareba et al., 2024a). As such, we identify a need for studies more finely delineating the elements of the guilt processing circuitry, with a particular importance placed on identifying the exact cognitive processes governed by specific brain regions and their connections.

Importantly, the current work suggests that approach-avoidance motivation might be one such factor. We observed increased left sATL activity in participants with greater approach towards their guilt memories, and elevated task-dependent coupling of the right sATL with ipsilateral paracentral and inferior parietal lobules in those with stronger avoidance. The potential functional differences between the bilateral sATL appear in line with some previous studies linking increased left sATL activity during social threat perception to lower levels of negative affectivity (Kret et al., 2011), and higher stress-related activity in the right ATL to maladaptive regulation strategies and stress-induced autonomic activity (Golde et al., 2023). Although the associations of increased left- and right-lateralised activity with, respectively, approach and avoidance motivation are predominantly related to the functioning of the frontal brain areas (Kelley et al., 2017), the sATL could be one of the driving forces behind these observations as it communicates the social conceptual information to the frontal regions through feedforward projections of the uncinate fasciculus (Sakata et al., 2019). Importantly for the avoidance-related results, the right sATL is also structurally connected to the ipsilateral paracentral and inferior parietal lobules (Fan et al., 2016). While the increased guilt-dependent connectivity with the former area might represent embodiment of the avoidance concept (Zhou et al., 2024), in the case of the right inferior parietal lobule the higher coupling might signify stronger integration of negative social feedback (Davis et al., 2023), and its contribution to the emergence of guilt-related avoidance (Gao et al., 2021).

Last but not least, the current work builds on the previous psychopharmacological studies demonstrating that manipulating neuromodulatory systems influences guilt and moral behaviour (Kanen et al., 2021; Li and Zu, 2024; Zheng et al., 2024), and hints at brain areas that could potentially mediate these effects. The role of 5-HT and OXT in guilt processing is likely related to their involvement in, respectively, punishment-related behavioural inhibition (Yee et al., 2021) and social affiliation (Feldman, 2012). Such functions fit in with the observations that decreasing

5-HT levels enhances the feelings of guilt in highly empathetic individuals (Kanen et al., 2021) while OXT administration leads to stronger feelings of guilt (Li and Zu, 2024), especially in low empathy individuals (Zheng et al., 2024). Despite the opposite associations between neurotransmitter levels and reported guilt, we observed a great overlap between regions whose activity was linked to normative levels of 5-HT molecules and OXTR in our study, including amygdala, hippocampus, anterior insula, medial prefrontal cortex and precuneus, with the first two areas exclusively linked to the two aforementioned systems. Importantly, the same set of areas was further implicated in empathy (Yarkoni et al., 2011), indeed making them promising candidates to mediate the effects reported previously in the literature. In addition to elucidating the neural circuitry through which 5-HT and OXT may affect guilt-related cognitions, our study suggests that NE and DA systems could similarly have a modulatory effect on feelings of guilt and associated brain activity, possibly through signalling arousal and salience pertaining to the guilt memories (Jordan, 2023; Gibbs et al., 2007).

Nevertheless, due to the use of external neuromolecular data, the discussed analysis has a purely hypothesis-generating character, and the presented results should be treated with caution. The reported associations are meant to guide future pharmaco-fMRI studies on guilt processing by demonstrating which brain areas are presumably affected by particular neuromodulatory systems. In the case of positive validation, however, the deployed methodological approach holds promise for personalised psychiatry, where use of patient-specific neuroimaging data could guide the choice of pharmacological treatment. Regarding the clinical implications of the findings, we also stress the subclinical characteristics of the current cohort. While such populations likely share the neural basis for their symptomatology with the diagnosed individuals (Besteher et al. 2017), we cannot exclude the possibility that these associations may become altered in patients with a longer history of disorder (Agorastos et al., 2020), and as such the reported results require replication in subjects meeting clinical diagnosis. The inclusion of the subclinical sample could also contribute to the lack of hypothesised findings for increased salience and avoidance towards guilt memories in highly anxious individuals. Regarding the motivational aspect of guilt memories, we additionally acknowledge the fact that the cross-sectional design deployed in our study to link it with indices of neural activity is likely characterised by lower statistical power compared to the approach based on within-subject comparisons, nevertheless, the distribution of individual participants' data precluded the use of the latter method. Last but not least, while we did not observe any sex-related differences in terms of neural patterns associated with guilt processing, we cannot exclude the fact that increasing the sample size and more equal balancing of sexes could reveal the presence of subtler neuroimaging effects, as we indeed observed the influence of this factor on some of the associated behavioural measures.

Conclusions

In summary, the current study links the self-blaming bias of subclinically anxious individuals with specific maladaptive patterns of behaviour, such as more pronounced self-attacking and hiding, as well as inability to disengage from self-focused cognitions when feeling negative emotions about oneself. On the neural level, these observations were paralleled by increased guilt-dependent functional connectivity between the left sATL and bilateral sgACC, suggestive of stronger contribution of guilt experiences to the self-worth and social affiliation computations performed in the latter area. Importantly, distinct neural characteristics pertaining to the bilateral temporal circuitry were modulated by the strength of participants' self-blaming emotions and the approach-avoidance motivation towards their guilt memories, highlighting the complex, multidimensional nature of the phenomenon, together with the crucial role the social semantic processing appears to play in it.

Funding

This publication forms part of the following research projects awarded to MV: Grant PID2021-127516NB-I00 funded by MICIU/AEI/10.13039/501100011033 and by “ERDF/EU”, Grant RYC2019-028370-I funded by MICIU/AEI/10.13039/501100011033 and by “ESF Investing in your future”, Grant CIAICO/2021/088 funded by Conselleria de Educación, Universidades y Empleo and Grant UJI-B2022-55 funded by Universitat Jaume I.

Data availability

The guilt recollection task, the neuroimaging analyses scripts and anonymised data from the MSAT task will be made available on a GitHub repository upon acceptance of the manuscript. (1) Statistical maps showing the main group effects and associations with anxiety, approach-avoidance motivation and salience for the guilt recollection task data, (2) the parcellation scheme used for investigating links between guilt-related activity and the normative amounts of neuromodulatory transporters and receptors, (3) and the resulting non-thresholded and thresholded cross-modality association maps are available in the following NeuroVault repository: https://neurovault.org/collections/21877/.

CRediT author statement

MRZ: Conceptualization, Methodology, Investigation, Formal analysis, Writing - Original Draft, Visualisation. IGG: Methodology, Resources, Investigation, Formal analysis, Writing - Review & Editing. MIM: Resources, Investigation, Writing - Review & Editing. RB: Conceptualization, Writing - Review & Editing. PH: Conceptualization, Writing - Review & Editing. MV: Supervision, Conceptualisation, Methodology, Investigation, Writing - Review & Editing.

Acknowledgements

We would like to thank Prof. Roland Zahn, Dr. Suqian Duan and Dr. Diede Fennema of King’s College London for kindly providing us with the MSAT task. We would also like to express our gratitude to Raphael Kaplan for his feedback on the guilt recollection task design, as well as Lidon Marin-Marin, Giacomo Tartaro and Marta Rodriguez Aramendia for their feedback on the translation of the MSAT task.

Disclosure statement

The authors report there are no competing interests to declare.

Ethical statement

All the procedures followed were in accordance with the ethical standards of the responsible committee on human experimentation (institutional and national) and with the Declaration of Helsinki (1975), and the applicable revisions at the time that this research was underway. Informed consent to be included in the study was obtained from all the participants. The study protocol was approved by the Universitat Jaume I Ethics Committee (CEISH/07/2022).

References

Agorastos A, Stiedl O, Heinig A, Sommer A, Hager T, Freundlieb N, Schruers KR, Demiralay C. Inverse autonomic stress reactivity in depressed patients with and without prior history of depression. J Psychiatr Res. 2020 Dec;131:114-118. doi: 10.1016/j.jpsychires.2020.09.016.

Apetroaia A, Hill C, Creswell C. Parental responsibility beliefs: associations with parental anxiety and behaviours in the context of childhood anxiety disorders. J Affect Disord. 2015 Dec 1;188:127-33. doi: 10.1016/j.jad.2015.08.059.

Baldassarri SR, Park E, Finnema SJ, Planeta B, Nabulsi N, Najafzadeh S, Ropchan J, Huang Y, Hannestad J, Maloney K, Bhagwagar Z, Carson RE. Inverse changes in raphe and cortical 5-HT1B receptor availability after acute tryptophan depletion in healthy human subjects. Synapse. 2020 Oct;74(10):e22159. doi: 10.1002/syn.22159.

Bates D, Mächler M, Bolker B, Walker S. Fitting Linear Mixed-Effects Models Using lme4. 2015 J Stat Softw 67(1), 1–48. doi: 10.18637/jss.v067.i01.
Beck AT. Thinking and Depression. I. Idiosyncratic content and cognitive distortions. Arch Gen Psychiatry. 1963 Oct;9:324-33. doi: 10.1001/archpsyc.1963.01720160014002.
Belfort-DeAguiar R, Gallezot JD, Hwang JJ, Elshafie A, Yeckel CW, Chan O, Carson RE, Ding YS, Sherwin RS. Noradrenergic Activity in the Human Brain: A Mechanism Supporting the Defense Against Hypoglycemia. J Clin Endocrinol Metab. 2018 Jun 1;103(6):2244-2252. doi: 10.1210/jc.2017-02717.
Beliveau V, Ganz M, Feng L, Ozenne B, Højgaard L, Fisher PM, Svarer C, Greve DN, Knudsen GM. A High-Resolution In Vivo Atlas of the Human Brain's Serotonin System. J Neurosci. 2017 Jan 4;37(1):120-128. doi: 10.1523/JNEUROSCI.2830-16.2016.
Beliveau V, Svarer C, Frokjaer VG, Knudsen GM, Greve DN, Fisher PM. Functional connectivity of the dorsal and median raphe nuclei at rest. Neuroimage. 2015 Aug 1;116:187-95. doi: 10.1016/j.neuroimage.2015.04.065.
Besteher B, Gaser C, Langbein K, Dietzek M, Sauer H, Nenadić I. Effects of subclinical depression, anxiety and somatization on brain structure in healthy subjects. J Affect Disord. 2017 Jun;215:111-117. doi: 10.1016/j.jad.2017.03.039.
Betts MJ, Cardenas-Blanco A, Kanowski M, Jessen F, Düzel E. In vivo MRI assessment of the human locus coeruleus along its rostrocaudal extent in young and older adults. Neuroimage. 2017 Dec;163:150-159. doi: 10.1016/j.neuroimage.2017.09.042.
Binney RJ, Hoffman P, Lambon Ralph MA. Mapping the Multiple Graded Contributions of the Anterior Temporal Lobe Representational Hub to Abstract and Social Concepts: Evidence from Distortion-corrected fMRI. Cereb Cortex. 2016 Oct 1;26(11):4227-4241. doi: 10.1093/cercor/bhw260.
Cândea DM, Szentagotai-Tătar A. Shame-proneness, guilt-proneness and anxiety symptoms: A meta-analysis. J Anxiety Disord. 2018 Aug;58:78-106. doi: 10.1016/j.janxdis.2018.07.005.
Cao H, Barber AD, Rubio JM, Argyelan M, Gallego JA, Lencz T, Malhotra AK. Effects of phase encoding direction on test-retest reliability of human functional connectome. Neuroimage. 2023 Aug 15;277:120238. doi: 10.1016/j.neuroimage.2023.120238.
Carver CS, White, TL Behavioral inhibition, behavioral activation, and affective responses to impending reward and punishment: The BIS/BAS Scales. J Pers Soc Psychol. 1994 67(2):319–333. doi: 10.1037/0022-3514.67.2.319.
Caspar EA, Ioumpa K, Keysers C, Gazzola V. Obeying orders reduces vicarious brain activation towards victims' pain. Neuroimage. 2020 Nov 15;222:117251. doi: 10.1016/j.neuroimage.2020.117251.
Chen G, Adleman NE, Saad ZS, Leibenluft E, Cox RW. Applications of multivariate modeling to neuroimaging group analysis: a comprehensive alternative to univariate general linear model. Neuroimage. 2014 Oct 1;99:571-88. doi: 10.1016/j.neuroimage.2014.06.027.
Cox RW. AFNI: software for analysis and visualization of functional magnetic resonance neuroimages. Comput Biomed Res. 1996 Jun;29(3):162-73. doi: 10.1006/cbmr.1996.0014.
Davis MM, Modi HH, Skymba HV, Finnegan MK, Haigler K, Telzer EH, Rudolph KD. Thumbs up or thumbs down: neural processing of social feedback and links to social motivation in adolescent girls. Soc Cogn Affect Neurosci. 2023 Feb 23;18(1):nsac055. doi: 10.1093/scan/nsac055.
Delamillieure P, Doucet G, Mazoyer B, Turbelin MR, Delcroix N, Mellet E, Zago L, Crivello F, Petit L, Tzourio-Mazoyer N, Joliot M. The resting state questionnaire: An introspective questionnaire for evaluation of inner experience during the conscious resting state. Brain Res Bull. 2010 Apr 5;81(6):565-73. doi: 10.1016/j.brainresbull.2009.11.014.
Diedrichsen J, Balsters JH, Flavell J, Cussans E, Ramnani N. A probabilistic MR atlas of the human cerebellum. Neuroimage. 2009 May 15;46(1):39-46. doi: 10.1016/j.neuroimage.2009.01.045.
Ding YS, Singhal T, Planeta-Wilson B, Gallezot JD, Nabulsi N, Labaree D, Ropchan J, Henry S, Williams W, Carson RE, Neumeister A, Malison RT. PET imaging of the effects of age and

cocaine on the norepinephrine transporter in the human brain using (S,S)-[(11)C]O-methylreboxetine and HRRT. Synapse. 2010 Jan;64(1):30-8. doi: 10.1002/syn.20696.
Duan S, Lawrence A, Valmaggia L, Moll J, Zahn R. Maladaptive blame-related action tendencies are associated with vulnerability to major depressive disorder. J Psychiatr Res. 2021 Nov 27;145:70-76. doi: 10.1016/j.jpsychires.2021.11.043.
Duan S, Valmaggia L, Fennema D, Moll J, Zahn R. Remote virtual reality assessment elucidates self-blame-related action tendencies in depression. J Psychiatr Res. 2023 May;161:77-83. doi: 10.1016/j.jpsychires.2023.02.031.
Dukart J, Holiga Š, Chatham C, Hawkins P, Forsyth A, McMillan R, Myers J, Lingford-Hughes AR, Nutt DJ, Merlo-Pich E, Risterucci C, Boak L, Umbricht D, Schobel S, Liu T, Mehta MA, Zelaya FO, Williams SC, Brown G, Paulus M, Honey GD, Muthukumaraswamy S, Hipp J, Bertolino A, Sambataro F. Cerebral blood flow predicts differential neurotransmitter activity. Sci Rep. 2018 Mar 6;8(1):4074. doi: 10.1038/s41598-018-22444-0.
Esteban O, Markiewicz CJ, Blair RW, Moodie CA, Isik AI, Erramuzpe A, Kent JD, Goncalves M, DuPre E, Snyder M, Oya H, Ghosh SS, Wright J, Durnez J, Poldrack RA, Gorgolewski KJ. fMRIPrep: a robust preprocessing pipeline for functional MRI. Nat Methods. 2019 Jan;16(1):111-116. doi: 10.1038/s41592-018-0235-4.
Fan L, Li H, Zhuo J, Zhang Y, Wang J, Chen L, Yang Z, Chu C, Xie S, Laird AR, Fox PT, Eickhoff SB, Yu C, Jiang T. The Human Brainnetome Atlas: A New Brain Atlas Based on Connectional Architecture. Cereb Cortex. 2016 Aug;26(8):3508-26. doi: 10.1093/cercor/bhw157.
Feldman R. Oxytocin and social affiliation in humans. Horm Behav. 2012 Mar;61(3):380-91. doi: 10.1016/j.yhbeh.2012.01.008.
Fennema D, Barker GJ, O'Daly O, Duan S, Carr E, Goldsmith K, Young AH, Moll J, Zahn R. Self-blame-selective hyper-connectivity between anterior temporal and subgenual cortices predicts prognosis in major depressive disorder. Neuroimage Clin. 2023;39:103453. doi: 10.1016/j.nicl.2023.103453.
Fernandes B, Newton J, Essau CA. The Mediating Effects of Self-Esteem on Anxiety and Emotion Regulation. Psychol Rep. 2022 Apr;125(2):787-803. doi: 10.1177/0033294121996991.
Fried EI, Nesse RM. Depression sum-scores don't add up: why analyzing specific depression symptoms is essential. BMC Med. 2015 Apr 6;13:72. doi: 10.1186/s12916-015-0325-4.
Frossard J, Renaud O. Permutation tests for regression, ANOVA, and comparison of signals: the permuco package. 2021 J Stat Softw 99, 1–32. doi: 10.18637/jss.v099.i15.
Gallezot JD, Nabulsi N, Neumeister A, Planeta-Wilson B, Williams WA, Singhal T, Kim S, Maguire RP, McCarthy T, Frost JJ, Huang Y, Ding YS, Carson RE. Kinetic modeling of the serotonin 5-HT(1B) receptor radioligand [(11)C]P943 in humans. J Cereb Blood Flow Metab. 2010 Jan;30(1):196-210. doi: 10.1038/jcbfm.2009.195.
Gao X, Yu H, Peng L, Gong X, Xiang Y, Jiang C, Zhou X. The mutuality of social emotions: How the victim's reactive attitude influences the transgressor's emotional responses. Neuroimage. 2021 Dec 1;244:118631. doi: 10.1016/j.neuroimage.2021.118631.
Gibbs AA, Naudts KH, Spencer EP, David AS. The role of dopamine in attentional and memory biases for emotional information. Am J Psychiatry. 2007 Oct;164(10):1603-9; quiz 1624. doi: 10.1176/appi.ajp.2007.06081241.
Gifuni AJ, Kendal A, Jollant F. Neural mapping of guilt: a quantitative meta-analysis of functional imaging studies. Brain Imaging Behav. 2017 Aug;11(4):1164-1178. doi: 10.1007/s11682-016-9606-6.
Golde S, Gleich T, Romund L, Stippl A, Pelz P, Raufelder D, Lorenz RC, Beck A. Adolescents' neural reactivity to acute psychosocial stress: dysfunctional regulation habits are linked to temporal gyrus response. Dev Psychopathol. 2023 Feb;35(1):332-344. doi: 10.1017/S0954579421000572.
González-García I, Visser M. A Semantic Cognition Contribution to Mood and Anxiety Disorder Pathophysiology. Healthcare (Basel). 2023 Mar 10;11(6):821. doi: 10.3390/healthcare11060821.

Gorgolewski K, Burns CD, Madison C, Clark D, Halchenko YO, Waskom ML, Ghosh SS. Nipype: a flexible, lightweight and extensible neuroimaging data processing framework in python. Front Neuroinform. 2011 Aug 22;5:13. doi: 10.3389/fninf.2011.00013.
Green S, Lambon Ralph MA, Moll J, Zakrzewski J, Deakin JF, Grafman J, Zahn R. The neural basis of conceptual-emotional integration and its role in major depressive disorder. Soc Neurosci. 2013;8(5):417-33. doi: 10.1080/17470919.2013.810171.
Green S, Lambon Ralph MA, Moll J, Deakin JF, Zahn R. Guilt-selective functional disconnection of anterior temporal and subgenual cortices in major depressive disorder. Arch Gen Psychiatry. 2012 Oct;69(10):1014-21. doi: 10.1001/archgenpsychiatry.2012.135.
Gryglewski G, Seiger R, James GM, Godbersen GM, Komorowski A, Unterholzner J, Michenthaler P, Hahn A, Wadsak W, Mitterhauser M, Kasper S, Lanzenberger R. Spatial analysis and high resolution mapping of the human whole-brain transcriptome for integrative analysis in neuroimaging. Neuroimage. 2018 Aug 1;176:259-267. doi: 10.1016/j.neuroimage.2018.04.068.
Halai AD, Welbourne SR, Embleton K, Parkes LM. A comparison of dual gradient-echo and spin-echo fMRI of the inferior temporal lobe. Hum Brain Mapp. 2014 Aug;35(8):4118-28. doi: 10.1002/hbm.22463.
Hansen JY, Shafiei G, Markello RD, Smart K, Cox SML, Nørgaard M, Beliveau V, Wu Y, Gallezot JD, Aumont É, Servaes S, Scala SG, DuBois JM, Wainstein G, Bezgin G, Funck T, Schmitz TW, Spreng RN, Galovic M, Koepp MJ, Duncan JS, Coles JP, Fryer TD, Aigbirhio FI, McGinnity CJ, Hammers A, Soucy JP, Baillet S, Guimond S, Hietala J, Bedard MA, Leyton M, Kobayashi E, Rosa-Neto P, Ganz M, Knudsen GM, Palomero-Gallagher N, Shine JM, Carson RE, Tuominen L, Dagher A, Misic B. Mapping neurotransmitter systems to the structural and functional organization of the human neocortex. Nat Neurosci. 2022 Nov;25(11):1569-1581. doi: 10.1038/s41593-022-01186-3.
Harris MA, Orth U. The link between self-esteem and social relationships: A meta-analysis of longitudinal studies. J Pers Soc Psychol. 2020 Dec;119(6):1459-1477. doi: 10.1037/pspp0000265.
Jaeckle T, Williams SCR, Barker GJ, Basilio R, Carr E, Goldsmith K, Colasanti A, Giampietro V, Cleare A, Young AH, Moll J, Zahn R. Self-blame in major depression: a randomised pilot trial comparing fMRI neurofeedback with self-guided psychological strategies. Psychol Med. 2023 May;53(7):2831-2841. doi: 10.1017/S0033291721004797.
Jenkinson M, Beckmann CF, Behrens TE, Woolrich MW, Smith SM. FSL. Neuroimage. 2012 Aug 15;62(2):782-90. doi: 10.1016/j.neuroimage.2011.09.015.
Jordan R. The locus coeruleus as a global model failure system. Trends Neurosci. 2024 Feb;47(2):92-105. doi: 10.1016/j.tins.2023.11.006.
Kaller S, Rullmann M, Patt M, Becker GA, Luthardt J, Girbardt J, Meyer PM, Werner P, Barthel H, Bresch A, Fritz TH, Hesse S, Sabri O. Test-retest measurements of dopamine D1-type receptors using simultaneous PET/MRI imaging. Eur J Nucl Med Mol Imaging. 2017 Jun;44(6):1025-1032. doi: 10.1007/s00259-017-3645-0.
Kanen JW, Arntz FE, Yellowlees R, Cardinal RN, Price A, Christmas DM, Apergis-Schoute AM, Sahakian BJ, Robbins TW. Serotonin depletion amplifies distinct human social emotions as a function of individual differences in personality. Transl Psychiatry. 2021 Feb 1;11(1):81. doi: 10.1038/s41398-020-00880-9.
Kas MJH, Penninx BWJH, Knudsen GM, Cuthbert B, Falkai P, Sachs GS, Ressler KJ, Bałkowiec-Iskra E, Butlen-Ducuing F, Leboyer M, Marston H, Luthman J, Mantua V. Precision psychiatry roadmap: towards a biology-informed framework for mental disorders. Mol Psychiatry. 2025 Aug;30(8):3846-3855. doi: 10.1038/s41380-025-03070-5.
Kelley NJ, Hortensius R, Schutter DJLG, Harmon-Jones E. The relationship of approach/avoidance motivation and asymmetric frontal cortical activity: A review of studies manipulating frontal asymmetry. Int J Psychophysiol. 2017 Sep;119:19-30. doi: 10.1016/j.ijpsycho.2017.03.001.

Kret ME, Denollet J, Grèzes J, de Gelder B. The role of negative affectivity and social inhibition in perceiving social threat: an fMRI study. Neuropsychologia. 2011 Apr;49(5):1187-1193. doi: 10.1016/j.neuropsychologia.2011.02.007
Lambon Ralph MA, Jefferies E, Patterson K, Rogers TT. The neural and computational bases of semantic cognition. Nat Rev Neurosci. 2017 Jan;18(1):42-55. doi: 10.1038/nrn.2016.150.
Lebreton M, Barnes A, Miettunen J, Peltonen L, Ridler K, Veijola J, Tanskanen P, Suckling J, Jarvelin MR, Jones PB, Isohanni M, Bullmore ET, Murray GK. The brain structural disposition to social interaction. Eur J Neurosci. 2009 Jun;29(11):2247-52. doi: 10.1111/j.1460-9568.2009.06782.x.
Lee C, Fernandes MA. Emotional Encoding Context Leads to Memory Bias in Individuals with High Anxiety. Brain Sci. 2017 Dec 27;8(1):6. doi: 10.3390/brainsci8010006.
Li Z, Xu M. Oxytocin enhances group-based guilt in high moral disengagement individuals through increased moral responsibility. Psychoneuroendocrinology. 2024 Oct;168:107131. doi: 10.1016/j.psyneuen.2024.107131.
Li CS, Potenza MN, Lee DE, Planeta B, Gallezot JD, Labaree D, Henry S, Nabulsi N, Sinha R, Ding YS, Carson RE, Neumeister A. Decreased norepinephrine transporter availability in obesity: Positron Emission Tomography imaging with (S,S)-[(11)C]O-methylreboxetine. Neuroimage. 2014 Feb 1;86:306-10. doi: 10.1016/j.neuroimage.2013.10.004.
Li Z, Xu M. Oxytocin enhances group-based guilt in high moral disengagement individuals through increased moral responsibility. Psychoneuroendocrinology. 2024 Oct;168:107131. doi: 10.1016/j.psyneuen.2024.107131.
Li Z, Tong L, Guan M, He W, Wang L, Bu H, Shi D, Yan B. Altered Resting-State Amygdala Functional Connectivity after Real-Time fMRI Emotion Self-Regulation Training. Biomed Res Int. 2016;2016:2719895. doi: 10.1155/2016/2719895.
Lythe KE, Moll J, Gethin JA, Workman CI, Green S, Lambon Ralph MA, Deakin JF, Zahn R. Self-blame-Selective Hyperconnectivity Between Anterior Temporal and Subgenual Cortices and Prediction of Recurrent Depressive Episodes. JAMA Psychiatry. 2015 Nov;72(11):1119-26. doi: 10.1001/jamapsychiatry.2015.1813.
Matuskey D, Bhagwagar Z, Planeta B, Pittman B, Gallezot JD, Chen J, Wanyiri J, Najafzadeh S, Ropchan J, Geha P, Huang Y, Potenza MN, Neumeister A, Carson RE, Malison RT. Reductions in brain 5-HT1B receptor availability in primarily cocaine-dependent humans. Biol Psychiatry. 2014 Nov 15;76(10):816-22. doi: 10.1016/j.biopsych.2013.11.022.
Mclatchie N, Giner-Sorolla R, Derbyshire SW. 'Imagined guilt' vs 'recollected guilt': implications for fMRI. Soc Cogn Affect Neurosci. 2016 May;11(5):703-11. doi: 10.1093/scan/nsw001.
Moll J, Krueger F, Zahn R, Pardini M, de Oliveira-Souza R, Grafman J. Human fronto-mesolimbic networks guide decisions about charitable donation. Proc Natl Acad Sci U S A. 2006 Oct 17;103(42):15623-8. doi: 10.1073/pnas.0604475103.
Monachesi B, Deruti A, Vaes J, Leoni P, Grecucci A. How sexual objectification marks the brain: fMRI evidence of self-objectification and its harmful emotional consequences. Neuroimage. 2024 Aug 15;297:120729. doi: 10.1016/j.neuroimage.2024.120729.
Morawetz C, Riedel MC, Salo T, Berboth S, Eickhoff SB, Laird AR, Kohn N. Multiple large-scale neural networks underlying emotion regulation. Neurosci Biobehav Rev. 2020 Sep;116:382-395. doi: 10.1016/j.neubiorev.2020.07.001.
Murrough JW, Czermak C, Henry S, Nabulsi N, Gallezot JD, Gueorguieva R, Planeta-Wilson B, Krystal JH, Neumaier JF, Huang Y, Ding YS, Carson RE, Neumeister A. The effect of early trauma exposure on serotonin type 1B receptor expression revealed by reduced selective radioligand binding. Arch Gen Psychiatry. 2011 Sep;68(9):892-900. doi: 10.1001/archgenpsychiatry.2011.91.
Murrough JW, Henry S, Hu J, Gallezot JD, Planeta-Wilson B, Neumaier JF, Neumeister A. Reduced ventral striatal/ventral pallidal serotonin1B receptor binding potential in major depressive disorder. Psychopharmacology (Berl). 2011 Feb;213(2-3):547-53. doi: 10.1007/s00213-010-1881-0.

Murty VP, Shermohammed M, Smith DV, Carter RM, Huettel SA, Adcock RA. Resting state networks distinguish human ventral tegmental area from substantia nigra. Neuroimage. 2014 Oct 15;100:580-9. doi: 10.1016/j.neuroimage.2014.06.047.
Oldfield RC. The assessment and analysis of handedness: the Edinburgh inventory. Neuropsychologia. 1971 Mar;9(1):97-113. doi: 10.1016/0028-3932(71)90067-4.
Peirce J, Gray JR, Simpson S, MacAskill M, Höchenberger R, Sogo H, Kastman E, Lindeløv JK. PsychoPy2: Experiments in behavior made easy. Behav Res Methods. 2019 Feb;51(1):195-203. doi: 10.3758/s13428-018-01193-y.
Picó-Pérez M, Radua J, Steward T, Menchón JM, Soriano-Mas C. Emotion regulation in mood and anxiety disorders: A meta-analysis of fMRI cognitive reappraisal studies. Prog Neuropsychopharmacol Biol Psychiatry. 2017 Oct 3;79(Pt B):96-104. doi: 10.1016/j.pnpbp.2017.06.001.
Pittenger C, Adams TG Jr, Gallezot JD, Crowley MJ, Nabulsi N, James Ropchan, Gao H, Kichuk SA, Simpson R, Billingslea E, Hannestad J, Bloch M, Mayes L, Bhagwagar Z, Carson RE. OCD is associated with an altered association between sensorimotor gating and cortical and subcortical 5-HT1b receptor binding. J Affect Disord. 2016 May 15;196:87-96. doi: 10.1016/j.jad.2016.02.021.
Radhakrishnan R, Matuskey D, Nabulsi N, Gaiser E, Gallezot JD, Henry S, Planeta B, Lin SF, Ropchan J, Huang Y, Carson RE, D'Souza DC. In vivo 5-HT6 and 5-HT2A receptor availability in antipsychotic treated schizophrenia patients vs. unmedicated healthy humans measured with [11C]GSK215083 PET. Psychiatry Res Neuroimaging. 2020 Jan 30;295:111007. doi: 10.1016/j.pscychresns.2019.111007.
Radhakrishnan R, Nabulsi N, Gaiser E, Gallezot JD, Henry S, Planeta B, Lin SF, Ropchan J, Williams W, Morris E, D'Souza DC, Huang Y, Carson RE, Matuskey D. Age-Related Change in 5-HT6 Receptor Availability in Healthy Male Volunteers Measured with 11C-GSK215083 PET. J Nucl Med. 2018 Sep;59(9):1445-1450. doi: 10.2967/jnumed.117.206516.
Sakata H, Kim Y, Nejime M, Konoike N, Miyachi S, Nakamura K. Laminar Pattern of Projections Indicates the Hierarchical Organization of the Anterior Cingulate-Temporal Lobe Emotion System. Front Neuroanat. 2019 Jul 31;13:74. doi: 10.3389/fnana.2019.00074.
Sanchez-Rangel E, Gallezot JD, Yeckel CW, Lam W, Belfort-DeAguiar R, Chen MK, Carson RE, Sherwin R, Hwang JJ. Norepinephrine transporter availability in brown fat is reduced in obesity: a human PET study with [11C] MRB. Int J Obes (Lond). 2020 Apr;44(4):964-967. doi: 10.1038/s41366-019-0471-4.
Sandiego CM, Gallezot JD, Lim K, Ropchan J, Lin SF, Gao H, Morris ED, Cosgrove KP. Reference region modeling approaches for amphetamine challenge studies with [11C]FLB 457 and PET. J Cereb Blood Flow Metab. 2015 Mar 31;35(4):623-9. doi: 10.1038/jcbfm.2014.237.
Sandiego CM, Matuskey D, Lavery M, McGovern E, Huang Y, Nabulsi N, Ropchan J, Picciotto MR, Morris ED, McKee SA, Cosgrove KP. The Effect of Treatment with Guanfacine, an Alpha2 Adrenergic Agonist, on Dopaminergic Tone in Tobacco Smokers: An [11C]FLB457 PET Study. Neuropsychopharmacology. 2018 Apr;43(5):1052-1058. doi: 10.1038/npp.2017.223.
Saricicek A, Chen J, Planeta B, Ruf B, Subramanyam K, Maloney K, Matuskey D, Labaree D, Deserno L, Neumeister A, Krystal JH, Gallezot JD, Huang Y, Carson RE, Bhagwagar Z. Test-retest reliability of the novel 5-HT1B receptor PET radioligand [11C]P943. Eur J Nucl Med Mol Imaging. 2015 Mar;42(3):468-77. doi: 10.1007/s00259-014-2958-5.
Savli M, Bauer A, Mitterhauser M, Ding YS, Hahn A, Kroll T, Neumeister A, Haeusler D, Ungersboeck J, Henry S, Isfahani SA, Rattay F, Wadsak W, Kasper S, Lanzenberger R. Normative database of the serotonergic system in healthy subjects using multi-tracer PET. Neuroimage. 2012 Oct 15;63(1):447-59. doi: 10.1016/j.neuroimage.2012.07.001.
Silk JS, Davis S, McMakin DL, Dahl RE, Forbes EE. Why do anxious children become depressed teenagers? The role of social evaluative threat and reward processing. Psychol Med. 2012 Oct;42(10):2095-107. doi: 10.1017/S0033291712000207.
Slifstein M, van de Giessen E, Van Snellenberg J, Thompson JL, Narendran R, Gil R, Hackett E, Girgis R, Ojeil N, Moore H, D'Souza D, Malison RT, Huang Y, Lim K, Nabulsi N, Carson RE,

Lieberman JA, Abi-Dargham A. Deficits in prefrontal cortical and extrastriatal dopamine release in schizophrenia: a positron emission tomographic functional magnetic resonance imaging study. JAMA Psychiatry. 2015 Apr;72(4):316-24. doi: 10.1001/jamapsychiatry.2014.2414.

Smith CT, Crawford JL, Dang LC, Seaman KL, San Juan MD, Vijay A, Katz DT, Matuskey D, Cowan RL, Morris ED, Zald DH, Samanez-Larkin GR. Partial-volume correction increases estimated dopamine D2-like receptor binding potential and reduces adult age differences. J Cereb Blood Flow Metab. 2019 May;39(5):822-833. doi: 10.1177/0271678X17737693.

Spielberger, C. D. (1989). State-Trait Anxiety Inventory: Bibliography (2nd ed.). Palo Alto, CA: Consulting Psychologists Press.

Thye M, Hoffman P, Mirman D. The neural basis of naturalistic semantic and social cognition. Sci Rep. 2024 Mar 21;14(1):6796. doi: 10.1038/s41598-024-56897-3.

Torrubia R, Ávila C, Moltó J, Caseras X. The Sensitivity to Punishment and Sensitivity to Reward Questionnaire (SPSRQ) as a measure of Gray's anxiety and impulsivity dimensions. Pers Individ Dif. 2001. 31:837–862. doi: 10.1016/S0191-8869(00)00183-5.

Wang Y, Chen X, Liu R, Zhang Z, Zhou J, Feng Y, Jiang C, Zuo XN, Zhou Y, Wang G. Effect of Phase-Encoding Direction on Gender Differences: A Resting-State Functional Magnetic Resonance Imaging Study. Front Neurosci. 2022 Jan 25;15:748080. doi: 10.3389/fnins.2021.748080.

Will GJ, Rutledge RB, Moutoussis M, Dolan RJ. Neural and computational processes underlying dynamic changes in self-esteem. Elife. 2017 Oct 24;6:e28098. doi: 10.7554/eLife.28098.

Woletz M, Hoffmann A, Tik M, Sladky R, Lanzenberger R, Robinson S, Windischberger C. Beware detrending: Optimal preprocessing pipeline for low-frequency fluctuation analysis. Hum Brain Mapp. 2019 Apr 1;40(5):1571-1582. doi: 10.1002/hbm.24468.

Yarkoni T, Poldrack RA, Nichols TE, Van Essen DC, Wager TD. Large-scale automated synthesis of human functional neuroimaging data. Nat Methods. 2011 Jun 26;8(8):665-70. doi: 10.1038/nmeth.1635.

Yee DM, Leng X, Shenhav A, Braver TS. Aversive motivation and cognitive control. Neurosci Biobehav Rev. 2022 Feb;133:104493. doi: 10.1016/j.neubiorev.2021.12.016.

Yuan K, Zheng YB, Wang YJ, Sun YK, Gong YM, Huang YT, Chen X, Liu XX, Zhong Y, Su SZ, Gao N, Lu YL, Wang Z, Liu WJ, Que JY, Yang YB, Zhang AY, Jing MN, Yuan CW, Zeng N, Vitiello MV, Patel V, Fazel S, Minas H, Thornicroft G, Fan TT, Lin X, Yan W, Shi L, Shi J, Kosten T, Bao YP, Lu L. A systematic review and meta-analysis on prevalence of and risk factors associated with depression, anxiety and insomnia in infectious diseases, including COVID-19: a call to action. Mol Psychiatry. 2022 Aug;27(8):3214-3222. doi: 10.1038/s41380-022-01638-z.

Zahn R, Moll J, Krueger F, Huey ED, Garrido G, Grafman J. Social concepts are represented in the superior anterior temporal cortex. Proc Natl Acad Sci U S A. 2007 Apr 10;104(15):6430-5. doi: 10.1073/pnas.0607061104.

Zahn R, Weingartner JH, Basilio R, Bado P, Mattos P, Sato JR, de Oliveira-Souza R, Fontenelle LF, Young AH, Moll J. Blame-rebalance fMRI neurofeedback in major depressive disorder: A randomised proof-of-concept trial. Neuroimage Clin. 2019;24:101992. doi: 10.1016/j.nicl.2019.101992.

Zahn R. The psychopathology of mood disorders: implications for identifying neurocognitive intervention targets. J Affect Disord. 2025 Sep 15;385:119423. doi: 10.1016/j.jad.2025.119423.

Zahn R, Lythe KE, Gethin JA, Green S, Deakin JF, Workman C, Moll J. Negative emotions towards others are diminished in remitted major depression. Eur Psychiatry. 2015 Jun;30(4):448-53. doi: 10.1016/j.eurpsy.2015.02.005.

Zakiniaeiz Y, Hillmer AT, Matuskey D, Nabulsi N, Ropchan J, Mazure CM, Picciotto MR, Huang Y, McKee SA, Morris ED, Cosgrove KP. Sex differences in amphetamine-induced dopamine release in the dorsolateral prefrontal cortex of tobacco smokers. Neuropsychopharmacology. 2019 Dec;44(13):2205-2211. doi: 10.1038/s41386-019-0456-y.

Zareba MR, Bielski K, Costumero V, Visser M. Graph analysis of guilt processing network highlights links with subclinical anxiety and self-blame. Soc Cogn Affect Neurosci. 2024a Dec 13;19(1):nsae092. doi: 10.1093/scan/nsae092.

Zareba MR, Ariño-Braña P, Picó-Pérez M, Visser M. Noradrenergic and Dopaminergic Neural Correlates of Trait Anxiety: Unveiling the Impact of Maladaptive Emotion Regulation. bioRxiv 2024b 2024.07.23.604801, doi: 10.1101/2024.07.23.604801.

Zareba MR, Davydova T, Palomar-García MÁ, Adrián-Ventura J, Costumero V, Visser M. Subjective sleep quality in healthy young adults moderates associations of sensitivity to punishment and reward with functional connectivity of regions relevant for insomnia disorder. Sleep Med. 2025 Jul;131:106527. doi: 10.1016/j.sleep.2025.106527.

Zheng X, Wang J, Yang X, Xu L, Becker B, Sahakian BJ, Robbins TW, Kendrick KM. Oxytocin, but not vasopressin, decreases willingness to harm others by promoting moral emotions of guilt and shame. Mol Psychiatry. 2024 Nov;29(11):3475-3482. doi: 10.1038/s41380-024-02590-w.

Zhou Q, Chen Y, Zhou C, Wang J. Long-term motor training enhances functional connectivity between semantic and motor regions in an effector-specific manner: evidence from elite female football athletes. Brain Struct Funct. 2024 Jul;229(6):1447-1459. doi: 10.1007/s00429-024-02808-1.

Zlomuzica A, Dere D, Machulska A, Adolph D, Dere E, Margraf J. Episodic memories in anxiety disorders: clinical implications. Front Behav Neurosci. 2014 Apr 24;8:131. doi: 10.3389/fnbeh.2014.00131.

Zou QH, Zhu CZ, Yang Y, Zuo XN, Long XY, Cao QJ, Wang YF, Zang YF. An improved approach to detection of amplitude of low-frequency fluctuation (ALFF) for resting-state fMRI: fractional ALFF. J Neurosci Methods. 2008 Jul 15;172(1):137-41. doi: 10.1016/j.jneumeth.2008.04.012.

Zuo XN, Di Martino A, Kelly C, Shehzad ZE, Gee DG, Klein DF, Castellanos FX, Biswal BB, Milham MP. The oscillating brain: complex and reliable. Neuroimage. 2010 Jan 15;49(2):1432-45. doi: 10.1016/j.neuroimage.2009.09.037.